

A single amino acid substitution in the NS4B protein of Dengue virus confers enhanced virus growth and fitness in human cells *in vitro* through interferon-dependent host response

Thuy Thu Bui^{1,2}, Meng LingMoi^{1, **}, Takeshi Nabeshima¹, Taichiro Takemura³, Trang Thu Nguyen³, Linh NgocNguyen⁴, Hang Thi Thu Pham⁴, Thi Thu ThuyNguyen⁴, Dao Huy Manh^{2,7}, Shyam Prakash Dumre⁷, Shusaku Mizukami⁸, Kenji Hirayama⁷, Shigeru Tajima⁶, Mai Thi Quynh Le⁴, Kiyoshi Aoyagi⁹, Futoshi Hasebe⁵, Kouichi Morita^{1,*}.

- 1) Department of Virology, Institute of Tropical Medicine, Nagasaki University, Nagasaki, Japan
- 2) Graduate School of Biomedical Sciences, Nagasaki University, Nagasaki, Japan
- 3) NIHE-Nagasaki Friendship Laboratory, Nagasaki University, Hanoi, Viet Nam
- 4) Department of Virology, National Institute of Hygiene and Epidemiology, Hanoi, Viet Nam
- 5) Vietnam Research station, Center for Infectious Disease Research in Asia and Africa, Institute of Tropical Medicine, Nagasaki University, Nagasaki, Japan
- 6) Department of Virology 1, National Institute of Infectious Diseases, Tokyo, Japan
- 7) Department of Immunogenetics, Institute of Tropical Medicine, Nagasaki University, Nagasaki, Japan
- 8) Department of Clinical Product Development, Institute of Tropical Medicine, Nagasaki University, Nagasaki, Japan
- 9) Department of Public Health, Nagasaki University Graduate School of Biomedical Sciences

Corresponding author:

*Kouichi Morita: moritak@nagasaki-u.ac.jp (Department of Virology, Institute of Tropical Medicine, Nagasaki University, Sakamoto 1-12-4, Nagasaki, Nagasaki 852-8523, Japan. Tel: +81-95-819-7829, Fax: +81-95-819-7830)

** Meng Ling Moi: sherry@nagasaki-u.ac.jp (Department of Virology, Institute of Tropical Medicine, Nagasaki University, Sakamoto 1-12-4, Nagasaki, Nagasaki 852-8523, Japan. Tel: +81-95-819-7829, Fax: +81-95-819-7830)

Abstract

Dengue virus (DENV) replication between mosquito and human hosts is hypothesized to be associated with viral determinants that interact in a differential manner between hosts. However, understanding of interhost viral determinants that drive DENV replication and growth between hosts is limited. Through the use of clinical isolates, we identified an amino acid variation of Ala, Met and Val at the position 116 of DENV-1 NS4B. While the proportion of virus with the NS4B-116V variant remained constantly high in serial passages in a mosquito cell line, populations of the NS4B-116M and NS4B-116A variants became dominant after serial passages in mammalian cell lines. Using recombinant DENV-1 viruses, the Val to Ala or Met alteration at the position NS4B-116 (rDENV-1-NS4B-116A and rDENV-1-NS4B-116M) resulted in enhanced virus growth in human cells in comparison to the clone with Val at NS4B-116 (rDENV-1-NS4B-116V). However, the reverse phenomenon was observed in mosquito cell line. Additionally, in a human cell line, differential levels of interferon- α/β and interferon stimulated-genes expressions (IFIT3, IFI44L, OAS1) suggested that the enhanced viral growth was dependent on the ability of the NS4B protein to hamper host interferon response during the early phase of infection. Overall, we identified a novel and critical viral determinant at the pTMD3 of NS4B region that displayed differential effects on DENV replication and fitness in human and mosquito cell lines. Taken together, the results suggest the importance of the NS4B protein in virus replication and adaptation between hosts.

Introduction

Dengue is one of the most common arthropod-borne (arbovirus) tropical diseases with millions of people affected every year. Dengue virus (DENV), the causative agent of this disease is transmitted to humans by a bite of *Aedes aegypti* or *Aedes albopictus* mosquito and causes a wide spectrum of clinical manifestation, ranging from mild fever to severe disease. The virus is a member of the *Flavivirus* genus belonging to the *Flaviviridae* family. The genome of the four serotypes of this virus (DENV1 to 4) is a positive-stranded RNA of approximately 11 kb [1, 2]. A viral precursor polyprotein translated from a single open reading frame (ORF) at 5' end of RNA genome is cleaved into three structural proteins (envelope [E], preMembrane [prM], and capsid [C]) and seven non-structural proteins (NS1, NS2A-NS2B, NS3, NS4A-NS4B, and NS5) through the protein processing [1]. The structural proteins are responsible for the formation of the viral particle while the non-structural proteins are components of the replication complex which are involved in the viral RNA synthesis, virion assembly, and antagonism of the immune response [1].

A rapid rate of genetic alteration was observed in RNA viruses because of the low fidelity of their RNA-dependent RNA polymerase, short replication time, and large population size. As a result, a population of quasi-species with closely-related sequences accumulates within an individual host [3]. Replication of DENV within host produces distinct virus populations at the host level, leading to the emergence of genetically distinct DENV genotypes and serotypes. Despite this, arboviruses, including DENV are unique among RNA viruses, in which the virus cycles between vertebrate and invertebrate hosts, resulting in the additional selective constraints as compared to other single-host RNA viruses [4][5]. The genetic stability of these viruses has been well-documented and is involved in their survival in distinct environments [6, 7]. It has been reported that mosquito vector may play an important role in the sequence conservation of DENV by maintaining a more homogenous viral population. Other investigators demonstrated that quasi-species of DENV population can be isolated from

the human host [8-11]. However, the role of quasi-species in DENV pathogenesis and inter-host interaction has yet to be fully understood.

In this study, following the isolation of viruses in different cell lines from dengue patient serum samples collected in the 2013 epidemic in Hue, Vietnam, we observe different amino acid residues at position 116 of the non-structural protein NS4B in DENV-1 populations isolated, including Valine (Val or V), Methionine (Met or M) and Alanine (Ala or A). Unlike the two enzymatic non-structural proteins NS3 and NS5 which are well characterized, the NS4B has no identified enzymatic activity and understanding on the functional role of the NS4B protein in host infection is limited [12, 13]. Previous studies have demonstrated that the biological function of NS4B is involved in host innate immunity and interaction with other non-structural proteins in the replication complex [14]. Despite the NS4B protein being highly conserved with 78% identity among the DENV serotypes and 97% within a serotype, the NS4B region is believed to possess a high tendency in developing adaptive mutations in response to different hosts [2].

In this study, we investigated the viral determinants that contributed to the fitness of the virus in different host cell lines. We demonstrated that the NS4B-116 Met/Ala amino acid at the position 116 in the NS4B region led to enhanced virus growth in human cells. In contrast, the Val residue at the position 116 of NS4B is vital for enhanced virus growth in mosquito cell lines. Our results suggest that Met and Ala variants at position 116 of the NS4B region may confer enhancement of viral growth in human cells through an interferon-dependent host response. The study thus highlights the importance of NS4B in DENV replication and in inter-host adaptation between human and mosquito hosts.

Results

Sequence comparison between 3 variants of isolated DENV-1 (NS4B-116Val, NS4B-116Ala, NS4B-116Met)

Strains of DENV serotype-1 (DENV-1) were isolated from serum samples of 15 patients in Hue, Vietnam in 2013, by parallel isolation in Vero and C6/36 mosquito cell lines. The isolated DENV-1 strains belonged to Genotype I and were closely related to those of DENV-1 strains isolated from Vietnam in 2007 (Genbank no. FJ182029), Taiwan in 2008 (Genbank no. AB608786), Cambodia in 2007 (Genbank no. FJ639688). The variants of DENV-1 strains isolated from the samples are listed in Table S1. These variants demonstrated a total of 9 different amino acids in 4 regions of the sequenced full genome (prM, NS2B, NS4A, NS4B). Notably, while virus isolates from 7 of the 15 DENV-1 patients obtained by inoculation of the patient serum specifically onto mosquito cells consistently possessed a Val residue (116V- encoded by codon GTG) at position 116 of the non-structural protein NS4B, isolates obtained from mammalian cells (Vero) possessed either at (116M- encoded by codon ATG) or a Ala (116A- encoded by codon GCG) residue (see Table S1). Because the isolates demonstrated consistent amino acid changes at the NS4B-116 position, we attempted to determine the role of nucleotide differences in the NS4B region. Of the 7 samples, one demonstrated the NS4B-116A variant (VN/2013/Hue/265) while the NS4B-116M variant was detected in 6 samples (VN/2013/Hue/338, 387, 432, 762, 817, and 988) (Table S1). The full genome sequence of VN/2013/Hue/265 isolated in C6/36 cells was submitted to GenBank (accession no. KX595191). Patients in all seven cases presenting with amino acid variations in the viruses isolated from them had dengue fever according to WHO classification [15].

The viral phenotypes with variants NS4B-116V, NS4B-116A, NS4B-116M were determined by using mammalian and mosquito cell lines. Because DENV cycles between the invertebrate and vertebrate hosts, to better reflect those of the natural transmission pattern and determine the influence of the hosts to the genetic change, alternate passages of the viruses

indifferent cell lines as well as serial passages in the same cell lines were performed. Two serum samples VN/2013/Hue/432 and VN/2013/Hue/265 that provided the variants were selected and passaged serially in (1) mosquito cell line (C6/36), (2) mammalian cell line (Vero) and (3) alternately between these two cell lines until 3 or 7 passages (Fig. 1). The number of passages was determined when the population of virus variants with NS4B-116A and 116M from the two samples surpassed 50%, at which each variant has reached a plateau in the population growth (here the percentage of NS4B-116A and 116M reached to 61% and 67%, respectively). Changes in the amino acid residues of the viruses at each passage are shown in Table 1. In the sample VN/2013/Hue/265, whole genome sequencing revealed that genome-wide consensus with the variant 116V of NS4B was maintained in all serial passages in C6/36 or in alternate passages between C6/36 and Vero cells. However, in serial passages in Vero cells, the NS4B-116V variant became dominant only at passage 1 (p1) and 2 of the viruses while the variant NS4B-116A was dominant at p3 and was maintained in subsequent passages (Table 1). By using deep sequencing and Sanger sequence chromatogram analyses, the results demonstrated that the amino acid residue at position 116 in these populations was a mixture of Ala and Val variants, in which one population predominated over the other (Table 1, Fig. S1a-c). Similarly, by using another DENV-1 patient sample (VN/2013/Hue/432), the presence of the variant NS4B-116M was noted to predominate after 2 serial passages in Vero cells (Table 1, Fig. S1e-g). To determine the proportion of each virus variant (NS4B-116V, NS4B-116M, NS4B-116A) in the virus population at each serial passage in Vero cells or alternate passage between Vero and C6/36 cells, a 3D-Digital PCR assay was performed. Initial passage of the clinical sample VN/2013/Hue/265 demonstrated that the population of NS4B-116A variant increased gradually from p1 to p7 in Vero cells (5.1% in passage 1, >50% in p3 and 67.1% in p7) (Table 1, Fig. S1d). Similarly, in sample VN/2013/Hue/432, the percentage of NS4B-116M virus exceeded 50% after two serial passages in Vero cells and reached 61% in p3 (Table 1, Fig. S1h). The variance in the population was confirmed by

using deep sequencing analyses. Interestingly, in alternate passages between Vero and C6/36 cells, the population of variant NS4B-116A was 5.1% at p1, then reached to 7.2% at p5 and 37% at p7, as determined by 3D-digital PCR and deep sequencing (Table 1, Fig. S1i-k).

Differential focus-forming morphology with NS4B-116Ala and NS4B-116Met versus NS4B-116 Val variants

To identify the determinants for growth characteristics and phenotype in cell culture, viruses isolated after the passages of two clinical samples (VN/2013/Hue/265 and VN/2013/Hue/432) mentioned above were used for the analyses of the morphology of the foci of infected cells. Small and homogenous foci were observed after infection and incubation of the cells with the viruses isolated at p1 in C6/36 and Vero cells of sample VN/2013/Hue/265, in which the variant NS4B-116V predominated over the NS4B-116A (Fig. 2a, b). Similar focus forming morphology was consistently observed when the virus inoculum was either from the 7th serial passages in C6/36 or alternate passages between C6/36 and Vero (Fig. 2c, e). In contrast, using the inoculum of isolates in which the NS4B-116A predominated over the NS4B-116V (p7 of serial Vero), the focus morphology was heterogeneous with the appearance of a mixture of large and smaller sized foci (Fig. 2d). Similarly, the inoculum from p7 of alternate passages between Vero and C6/36 cells in which 37% of the population consisted of the variant NS4B-116A caused the appearance of big foci together with the smaller ones (Fig. 2f). The sample VN/2013/Hue/432 also resulted in the appearance of large and small foci at p2 and 3 of serial passages in Vero cells while foci of cells infected with DENV at p1 in either C6/36 or Vero cells, and at p3 in C6/36 cells remained small (Fig. 2g-j). Foci size correlates with the predominance of one variant over the other, in which predominant viruses with variants NS4B-116M/A resulted in a higher proportion of foci with large size as compared to those populations with a predominance of NS4B-116V. The results suggest the notion that the amino acid at the position of 116 of the NS4B region plays a critical role in viral replication.

Using a DENV-1 infectious clone (rDENV-1-NS4B-116V) with the amino acid residue of 116V in NS4B as a template, we further generated two mutant infectious clones which possessed the amino acid V116M and V116A substitution in this region. The focus forming phenotype was also confirmed in the two mutant recombinant viruses, rDENV-1-NS4B-116A, and rDENV-1-NS4B-116M. The two recombinant viruses (rDENV-1-NS4B-116A, and rDENV-1-NS4B-116M) produced foci with mean diameters of 0.83 ± 0.04 mm and 0.79 ± 0.03 mm, respectively, the sizes of which were double than those produced by the rDENV-1-NS4B-116V clone (0.37 ± 0.02 mm) ($p < 0.0001$) (Fig.2k-m). Moreover, the two clones (rDENV-1-NS4B-116A and rDENV-1-NS4B-116M) showed significantly bigger plaque formations with the mean diameters of 1.54 ± 0.07 mm and 1.55 ± 0.23 mm, respectively as compared to those plaques formed due to the rDENV-1-NS4B-116V clone (0.97 ± 0.13 mm) ($P < 0.05$) (Fig.2n-p). The focus-forming phenotype of the infectious-clone of each virus strain recapitulated those of clinically-derived isolates. The results suggest that the nucleotide differences in the NS4B region account for the differential viral phenotypes in mammalian and mosquito cell lines.

The V116A and V116M substitution enhances virus growth in human cell lines but not in a mosquito cell line

To determine the role of the amino acid variants at the position 116 of DENV-1 NS4B, the growth kinetics of two infectious clones (rDENV-1-NS4B-116A and rDENV-1-NS4B-116M) with a single mutation at that residue and the virus clone rDENV-1-NS4B-116V were compared in different cell lines. The recombinant viruses were inoculated onto a mosquito cell line C6/36 (*Aedes albopictus* mosquito cells); human cell lines namely K-562 (human myelogenous leukemia cells), immature iPS-ML dendritic-like cells and Hep G2 (human liver hepatocellular cells); and mammalian cell line Vero (Green monkey-kidney cells). The virus titres of the infectious virus in the culture supernatant were assessed at various time points (Fig.3). Although both clones replicated in these cell lines, the growth patterns were different

between the three infectious clones in mosquito and human cells. In C6/36 cells, the infectious clone rDENV-1-NS4B-116V replicated rapidly as compared to the two mutants rDENV-1-NS4B-116A and rDENV-1-NS4B-116M from day 4 post-infection (p.i.) (Fig. 3a). The virus titre of rDENV-1-NS4B-116V at 6 days p.i. was approximately 10 times higher ($1.15 \log_{10} - 1.13 \log_{10}$) as compared to those with Ala and Met substitutions (NS4B-116A and 116M) ($P < 0.05$) (Fig. 3a). In contrast, virus titres of these two infectious clones in human cells were higher as compared to that of the rDENV-1-NS4B-116V clone at various time points. In K-562 cells, the rDENV-1-NS4B-116A and rDENV-1-NS4B-116M infectious clones replicated at a rapid rate, approximately 10 times higher than that of rDENV-1-NS4B-116V clone ($P < 0.05$) (Fig. 3b). In immature iPS-ML-DC cells, the virus titres of the two infectious clones with Ala and Met substitutions were significantly higher from day 1 p.i. as compared to that of rDENV-1-NS4B-116V virus ($P < 0.05$) (Fig. 3c). Similarly, the two infectious clones rDENV-1-NS4B-116A and rDENV-1-NS4B-116M also showed a significant increase in virus titres (at least 1 \log_{10} higher) at 3 and 4 days p.i. in Hep G2 when compared to the virus clone rDENV-1-NS4B-116V ($P < 0.05$) (Fig. 3d). However, the growth kinetics of the three clones showed no differences at all incubation time points in Vero cells (Fig. 3e). Overall, the growth kinetics of the two infectious clones with Ala and Met substitutions at the NS4B-116 position demonstrated significantly lower virus titres in mosquito cells (C6/36). Furthermore, virus titres in human cell lines (K-562, immature iPS-ML-DCs and Hep G2) were significantly higher as compared to that of the infectious clone with NS4B-116-Val.

The NS4B-V116A and V116M confers enhanced fitness of DENV-1 in human cell lines

We further examined the role of Val residue of the NS4B-116 in virus replication between different hosts. Here, we determined the relative fitness of NS4B-116V, NS4B-116A and NS4B-116M *in vitro* using co-infection of either rDENV-1-NS4B-116V and rDENV-1-NS4B-116A or rDENV-1-NS4B-116V and rDENV-1-NS4B-116M in a human cell line (Hep G2) and a mosquito cell line (C6/36) (Fig 4). A single virus clone was infected in parallel as a

control. The competition assay performed in mammalian cells (HepG2) demonstrated that the proportion of virus clones with Met and Ala residues at position NS4B-116 increased with serial passages. In the virus mixture that consists of rDENV-1-NS4B-116V and 116A, the proportion of rDENV-1-NS4B-116A clone increased from 8.9 % at the time of inoculation to 11.7 % at p1 and 66.5% at p3. In contrast, the population of clone rDENV-1-NS4B-116V declined significantly from 91.1% to 33.5% (Fig. 4a). Similarly, rDENV-1-NS4B-116M clone increased from 10 % in the inoculation mixture to 74.9 % at p1 and 96.9 % at p2 in the virus mixture that consisted of rDENV-1-NS4B-116V and 116M (Fig. 4b). Interestingly, a reverse pattern was observed after serial passages in mosquito cells, in which the recombinant virus clone rDENV-1-NS4B-116V became the dominant clone after serial passages (Fig. 4c,d). Starting from ratio 10:1 in the inoculation mix (rDENV-1-NS4B-116A/ M: rDENV-1-NS4B-116V), the rDENV-1-NS4B-116V clone rapidly reached to more than 50% of the virus population and became predominant in the virus population from the first passage (Fig. 4c,d). Overall, the viral fitness for rDENV-1-NS4B-116A and rDENV-1-NS4B-116M was enhanced in human cells but was reduced in mosquito cell line. In contrast, the rDENV-1-NS4B-116V clone demonstrated lower fitness levels in human cells but higher fitness levels in mosquito cells. These results are thus consistent with the data obtained from the clinical isolates and demonstrate that the Val/Ala/Met variants in NS4B protein 116 residue enhances viral growth in a host species-dependent manner. Interestingly, single clone infection constantly demonstrated homogenous virus population in all serial passages, suggesting that nucleotide differences did not arise from a spontaneous mutation in cell culture passages.

Levels of IFN α / β and transcriptional signatures of immature iPS-ML-DCs infected with rDENV-1

DENV has been hypothesized to target dendritic cells *in vivo* [16, 17]. Hence, in this study, we conducted gene microarray to determine differentially expressed genes (DEGs) in a human dendritic cell, immature iPS-ML-DCs. DEGs in cells infected with three DENV-1

infectious clones at various time points were compared to the control (non-infected). A hierarchical clustering with fold change ≥ 2 revealed 112DEGs were induced upon DENV infection as compared to the control ($P < 0.05$) (Fig. 5a-c). Genes associated with interferon regulation including CCL3, CCL4, IL6 were significantly up-regulated at the early phase of infection (Fig. 5d-e and more details in Table S3a). Interestingly, the transcripts of some interferon-stimulated genes (ISGs) such as IFIT3, IFI44L, and OAS1 in cells infected with rDENV-1-NS4B-116V were expressed at higher levels at 30 min p.i. (up-regulation) as compared to the levels of these transcripts expressed in cells infected with rDENV-1-NS4B-116A and rDENV-1-NS4B-116M clones (down-regulation) (Fig. 5e). However, not all ISGs such as IFITM1, IFIT5 showed the difference in the expression at this time point in the cells infected with rDENV-1-NS4B-116A/M versus rDENV-1-NS4B-116V (Table S3a). After 24h p.i. of cells infected with rDENV-1-NS4B-116M and rDENV-1-NS4B-116A clones, the levels of these ISGs increased to levels higher than those in cells infected with rDENV-1-NS4B-116V (Fig. 5f and Table S3a). All these transcripts remained at the same level of expression at the early time point (Fig. 5d and Table S3a). To support this observation, the levels of IFN type I in the infected culture supernatants were examined. Interestingly, while the levels of IFN- α in the supernatants of rDENV-1-NS4B-116A/M/V infected cells showed no significant difference at all time points, the levels of IFN- β secreted from the cells infected with rDENV-1-NS4B-116M and rDENV-1-NS4B-116A at 30 min p.i. and 48h p.i. were nearly two-fold lower than those with rDENV-1-NS4B-116V ($P < 0.05$) (Fig. 5g-h). A reverse trend was seen at 24h p.i., indicating the consistent correlation between regulation of IFN-type I and ISGs transcription. Additionally, genes responsible for the ubiquitination process, such as UBE2C and HERC5, were up-regulated in cells infected with rDENV-1-NS4B-116A and rDENV-1-NS4B-116M as compared to those in rDENV-1-NS4B-116V infected cells (Fig. 5 e-f) at 30 min p.i. and 24h p.i. The transcription signature patterns of ISGs including

IFIT2,3, IFITM1,3 and ubiquitination-related genes including UBE2C, HERC5,6 infected with three virus clones were also consistently observed in HepG2 cells (Table S3b).

Discussion

The diversity in the genome sequences of a virus within an individual host or among hosts termed as quasispecies is well-documented for many species of viruses such as HIV, HBV and in limited cases of DENV [8-11, 18-20]. It has been hypothesized that viral determinants are vital in DENV intra-host adaptability and virulence. In this study, DENV isolates containing the variants 116V and 116A of the NS4B were isolated from a single patient (VN/2013/Hue/265). Similarly, isolates containing NS4B-116V and 116M were obtained from another patient (VN/2013/Hue/432). Virus populations comprising NS4B-116A or NS4B-116M were observed in serial passages in Vero cells and/or alternate passages between Vero and C6/36 cells, in which the NS4B-116A/M population was dominant in early serial passage (p2-3) in Vero but remained the minor population at higher passage (p7) after alternate passages between Vero and C6/36 cells (Table 1). Although spontaneous mutations may occur in RNA virus due to the low fidelity of its RNA-dependent RNA polymerase during replication [21, 22], our results indicated that the NS4B-116A and NS4B-116M variants were present in clinical samples during virus isolation. Additionally, amino acid substitutions in the NS4B-116 position were absent in the multiple serial passages we conducted using homologous recombinant viruses in which rDENV-1-NS4B-116V was passaged in Vero cells and rDENV-1-NS4B-116A and rDENV-1-NS4B-116M were passaged separately in C6/36 cells (data not shown). Moreover, isolates obtained from sample VN/Hue/2013/265 by serial passages in Vero or alternate passages between Vero and C6/36 cells showed a mixture of two amino acids NS4B-116A and NS4B-116V from early passages (Table 1, Fig.S1). Together, these results indicate that the variants NS4B-116A and 116M originated from clinical samples rather than as a result of cell passage. The results also demonstrate that serial passages in C6/36 cells and alternate passages between C6/36 and Vero cells resulted in constantly low populations of these variants. In contrast, these variants accumulated serially in mammalian cells and alternate passages between mammalian and

mosquito cell lines. These results concur with the concept that alternate virus cycling between vertebrate and invertebrate hosts is vital in the evolutionary stability of DENV and other arboviruses [21, 23, 24]. As with other arboviruses, the evolutionary speed of DENV is relatively slower as compared to other RNA viruses due to cycling host transmission patterns, which further leads to additional selective constraints [4, 5, 25]. The effects of variants of the NS4B-116 residue (116A/M/V) in different host cell lines suggest two competing effects of the substitutions: one that would enhance growth in mammalian hosts but also would hamper growth in mosquito host. The results also concur with the hypothesis that supports the need for virus evolution to compromise strains in order to maximize survival outcomes in disparate environments of vertebrate and invertebrate. This, however, does not maximize fitness in either host [26].

NS4B is an integral membrane protein that associates with other non-structural proteins to form the replication complex and, as such, plays an essential role in the viral replication [27, 28]. Studies on the secondary structure of DENV-2 NS4B revealed five predictable transmembrane domains (pTMD 1-5) [29-31]. According to topology analyses, the residue 116 is located at the pTMD 3 of NS4B (residue 101-129) and spanned between the membrane of endoplasmic reticulum (ER) from the lumen to the cytoplasm of the host cell (Fig. 6a). The 116V residue of NS4B is conserved between DENV-1, 2, 3 serotypes but varied in DENV-4 serotype (Fig. 6b). However, due to the differences in length of 2K signal sequence at N-terminal of NS4B between the four serotypes, the residue 116V in NS4B DENV-1 is indicated as 115V in DENV 2,3 and 112L in DENV-4 (Fig. 6b). Previous investigators have reported that together with the K122I residue of the envelope protein, the NS4B-V115A residue in DENV-2 acts as a variable site that may contribute to increased virulence in mice *in vivo* [22, 32]. In the same NS4B domain 3, a Pro-to-Leu substitution in amino acid 101 of a rDENV-4 NS4B protein (NS4B P101L) is responsible for small foci phenotype in C6/36 cells and large foci in Vero and Huh-7 cells. This mutation decreases

DENV infectivity in mosquito host and also significantly restricts the infection in the midgut of intact mosquitoes [26]. Similarly, the amino acid substitutions in DENV-4 NS4B V109A, G119S, L112F and DENV-1 NS4B T109I, L113F have been shown to be responsible for the enhancement of the replication of the virus in Vero cells [22, 33]. Overall, our results also suggest that these substitution-mediated enhancements of viral replications were host-specific as shown by the improved growth of DENV-1 in human cells (K-562, Hep G2, and immature iPS-ML-DCs) but decreased growth in C6/36 cells (Fig. 3). Taken together, our results imply that the domain-3 of NS4B region has a higher tendency to develop mutations that may act as a “trade-off” role which reduces infectivity in mosquito host but enhances the replication in the human host.

Previous studies have demonstrated that the first 125 amino acids of DENV-2 including residue 77 to 125 of the NS4B region served as interferon- α/β (IFN) antagonists [14, 34, 35]. The expression of DENV-2 NS4B was believed to regulate the IFN- β signaling pathway via inhibiting the STAT1 phosphorylation, resulting in suppressed ISGs expression [35]. In this study, although no difference was observed in the levels of IFN- α , the levels of IFN- β secreted by cells infected with rDENV-1-NS4B-116A and rDENV-1-NS4B-116M were significantly lower than that with rDENV-1-NS4B-116V. These results indicate that the variant NS4B 116A/M associated with IFN- β antagonism of NS4B during the early phase of infection. In the present study, the differences in the regulation of ISGs in iPS-ML-DCs cells (OAS1, IFIT3, and IFI44L) at 30 min p.i. suggested a correlation between the differences in the growth kinetics of the three virus clones and the activity of ISGs. It was consistent with the proposal of previous investigators that these genes were for viral replication [36]. Our data on HepG2 cells also revealed that some ISGs including IFIT2,3, IFITM1,3 followed the same pattern of expression as OAS1, IFIT3, and IFI44L in iPS-ML-DCscells. At 24h p.i., the transcription of these ISGs in the cells infected with rDENV-1-NS4B-116V was lower than that of rDENV-1-NS4B-116A/M, indicating that the effects of the variant NS4B-116 A/M

were short-term and dependent on the time of infection. Collectively, the results indicated that the differential expression of ISGs may depend on the virus strain and host cells. The results concurred with the hypothesis that NS4B-associated IFN- α/β signaling transduction is conserved among human cell lines [34, 35]. In this study, the transcription of STAT1 remained the same at 5 min p.i., 30 min p.i. and differed at 24 h p.i. (Table S3a). Further studies are expected to address whether differential STAT1 levels and IFN- α/β response are due to down-regulation of STAT1 gene transcription or protein synthesis, protein phosphorylation or an enhanced degradation of the STAT protein in the cells infected by three virus variants. Additionally, in the replication complex, the interaction between NS1, NS3, NS4A, and NS4B are necessary for the early synthesis of viral RNA [27, 28, 37, 38]. Recent studies on the interaction between NS1 and NS4B has demonstrated that this binding can be interfered by the ubiquitination of NS1. The ubiquitination of viral protein is hypothesized to result in enhanced virus replication [38]. Further studies are needed to address whether the differences in the expression levels of ubiquitin-conjugating enzyme E2C gene (UBE2C) and E3 ubiquitin protein ligase 5,6 (HERC5,6) between cells infected with viruses harboring NS4B-116 variants are associated with the ubiquitination of non-structural proteins.

Previous studies have demonstrated that the DENV NS4A and NS4B synergistically function to mediate membrane rearrangement [28, 33]. The substitution P101L in pTMD3 of DENV-4 NS4B results in abrogation of the interaction between NS4B and NS3 [27]. In this study, although the variant NS4B-116A/M accumulated in Vero cells, these variants were not able to enhance the virus growth as compared to the virus clone with NS4B-116V. In regards to the differences in the characteristics between non-human mammalian cells (Vero cells) and human cells (K-562, HepG2, iPS-ML-DCs cells), the results suggest that the NS4B may function in a manner which is dependent on the host and viral factors. The NS4B-116A/M variations in the pTMD3 might contribute to the changes in the interaction between NS4B, NS3, and NS4A, and thus allows disassociation of the NS3 from the single-stranded viral

RNA by increasing of unwinding activity of NS3, or by altering cytoplasmic membrane rearrangement [27, 33]. In the NS4B, three domains of pTMD 3-5 of NS4B span through the ER membrane, indicating that this nonstructural protein may act as an anchor to secure the replication complex to the membrane [39]. Collectively, this implies that in a competitive environment (i.e. virus population with two variants in competition), variant which elicits conformational changes in replication complex may alter the ability of NS4B to attach the membrane to facilitate viral replication and accumulation of virus particles within host cells. However, further studies on the secondary structure of NS4B are needed to address the effects of these variations on viral protein structure and interaction of NS4B with other non-structural proteins, and growth outcomes.

Overall we identified a novel critical viral determinant at the pTMD3 of NS4B region that displayed differential effects on DENV replication and fitness human and mosquito cell lines. Interestingly, NS4B substitutions (NS4B-116A and NS4B-116M) increased virus growth in human cells but reduced significantly the viral replication in mosquito cells. In contrast, NS4B-116V substitution showed increased viral replication in mosquito cells as compared to human cell lines. Furthermore, our results imply that the differential virus growth between the NS4B-116A/M and V residue in a human cell line is associated with the interferon-dependent response. Taken together, the results suggest the importance of the NS4B protein in virus replication and adaptation in the specific host. Thus, in providing further understanding the role of NS4B in intra-host replication, our findings may be of interest in the identification of DENV strains with altered replication between hosts and offer a basis for the selection of attenuated vaccine candidates and potential therapeutics.

Methods

Sample collection.

The serum samples and clinical data were collected from dengue suspected patients admitted to Hue Central Hospital, Vietnam in 2013 who had developed the illness within 5 days of the disease onset. The diagnosis of dengue infection of these patients was based on WHO classification[15].

Cells.

African green monkey kidney (Vero) cells, human liver hepatocellular cells (Hep G2) and *Aedes albopictus* (C6/36) mosquito cells were grown in Eagle's Minimum Essential medium (MEM) with 10% fetal calf serum (FCS) and 1% penicillin and streptomycin (PS). Vero and Hep G2 cells were incubated at 37°C with 5% CO₂ whereas C6/36 cells were incubated at 28°C without CO₂. The human leukemic cell line K-562 was maintained or seeded in Biocoat Poly D-lysine flask or 24 well plate (Corning, ME) containing 10% FCS-RPMI and 1% PS and was incubated at 37°C with 5% CO₂ supply. The immature iPS cell-derived dendritic cell-like cells (immature iPS-ML-DCs) were originally differentiated from myeloid (iPS-ML) cells which were generated from human induced pluripotent stem (iPS) cells according to the previously established procedure with some modifications in the differentiation process [40]. Briefly, iPS-ML cells were maintained in MEM with 20% Fetal bovine serum (FBS), 1% PS, 12.5 ng/ml recombinant human (rh) M-CSF (Shenandoah Biotechnology, PA), 50 ng/ml rhGM-CSF (Gentaur, CA) and 10 ng/ml rhIL-4 (Humanzyme, IL) at 37°C, 5% CO₂ supply. Immature iPS-ML-DCs was generated by a 3-day culture in complete α -MEM with rM-CSF (12.5 ng/mL), rGM-CSF (100 ng/mL) and rhIL-4 (10 ng/mL) at 37°C, 5% CO₂.

Virus isolation and passages

To isolate the viruses from the serum samples of dengue suspected patient samples, a 10 μ l volume from each sample was inoculated in a monolayer culture of Vero and C6/36 cells, which were then maintained in 2% FCS-MEM for 6 days. A 100 μ l volume of culture fluids

from infected cells was used as inoculum in the subsequent second and third passage in these cell lines under the same conditions.

In order to determine the influence of the host to the genetic change of DENV *in vitro*, two serum samples VN/2013/Hue/265 (containing the variant NS4B-116A) and VN/2013/Hue/432 (containing the variant NS4B-116M) were selected for further passages in cell culture. DENV was serially passaged in mammalian cells (Vero) and mosquito cells (C6/36) or alternately passaged between two cell lines for a total of 3 or 7 passages. Initially, 10 µl of the serum sample was inoculated in an ~80% confluent 6 wells plates of Vero and C6/36. After 6 days of incubation, each of the collected infected culture fluid was sub-cultured for further alternate passages or serial passages to mammalian and mosquito cells at a constant MOI of 0.1 (Fig. 1). Viruses in each passage were harvested after 4 days p.i.

RNA extraction, amplification, and sequencing

DENV RNA from serum or cell culture supernatant was extracted by QIAmp viral RNA mini kit (Qiagen, Hilden, Germany). The serotypes of DENV in all serum samples were determined by Sanger sequencing method using the amplicon of E region amplified by dengue-consensus primers (Table S2). To determine the nucleotide sequence of the NS4B gene, a 500bp fragment of this region was amplified by using a primer set of DENV-1 (Table S2).

Sanger sequencing and Next Generation Sequencing.

The sequences of E and NS4B genes or the whole genome was conducted by either the Sanger method or Next-generation sequencing (NGS). To determine the whole sequence of dengue virus by NGS, cDNA libraries were constructed by Ion Total RNA-Seq Kit v2 (Life technologies, Lithuania) and then sequenced by using Ion Proton Sequencer (Life technologies). The De novo assembly was conducted by Trinity ver. 2.3.2. The assembled contigs were queried by NCBI-Blast+ ver.2.5.0 to search the most similar reference sequence of DENV. Reads from NGS were mapped to the reference sequence using BWA ver. 0.7.17.

A consensus sequence was built by Samtools ver.1.3 and the variants were called by Varscan ver 2.4.3.

Primers used for full genome sequencing are shown in Table S2. The results were assembled and analyzed by Codoncode aligner (CodonCode) and CLC Sequence viewer (Qiagen).

Virus titre quantification.

The DENV-1 genome copies were determined by quantitative real-time RT-PCR. TaqMan® Fast Virus 1-Step Master Mix (Life Technology, CA) was used for the reaction with E-realttime primer and probe set (Table S2). Thermal cycling was performed according to the manufacturer's instruction.

Quantification of the variant population by 3D-digital PCR

To determine the percentage of each of the variant 116A or 116M in the mixture with 116V, 3D digital PCR was conducted by using cDNA template with a point-mutation-specific probes (Denv1NS4B-mut116A/M and Denv1NS4B-wt116V probe) and primers (NS4B-forward and reverse) designed for each variant (Table S2). A quantity of 10-100ng of the cDNA generated from RNA was added to the reaction mix including the Quanstudio 3D Digital PCR reagent kit (Applied Biosystems, Pleasanton, CA) and two probes Denv1NS4B-mut116A/M, Denv1NS4B-wt116V. The reaction mix was loaded onto the chip (Applied Biosystems, CA) and the thermal cycling was done following the manufacturer's instruction. The data collected from chips were analyzed by Quant Studio 3D Analysis Suite cloud (Applied Biosystems). The results were presented as the percentage of 116A or 116M in the virus population. Due to the limited amount of samples, assays using these clinical samples could not be repeated.

Infectious DENV-1 clone and site-directed mutagenesis

A plasmid with the full genome of DENV-1(02-20)/pW119 (accession no. AB178040) was used [41]. The original infectious clone plasmid carried the amino acid Val at position

116 of NS4B. To generate two mutant clones with a single mutation of NS4B-116 Ala or Met from the original plasmid rDENV-1(02–20)/pMW119 (rDENV-1-NS4B-116V) by site-directed mutagenesis PCR, primer setDenv1NS4B mut116A 7137 was used to introduce a V116A substitution and primer setDenv1NS4B mut116M 7137 was used to introduce a V116M substitution (Table S2). The PCR products amplified by *Pfu* Turbo DNA Polymerase kit (Agilent Technology) were then treated with DpnI to digest plasmid templates, purified, self-ligated and transformed into *E.coli* strain Stb12 (Invitrogen) [41]. Finally, two plasmids rDENV-1-NS4B-116A/pMW119 and rDENV-1-NS4B-116M/pMW119 were generated.

***In vitro* RNA synthesis and RNA transfection**

Transcribed RNA of the three plasmids rDENV-1-NS4B-116A/pMW119, rDENV-1-NS4B-116M/pMW119, and rDENV-1-NS4B-116V/pMW119 were generated according to the established procedure by using mMACHINE RNA transcription kit (Ambion, TX) [41]. A total of 3-4 µg of purified RNA was transfected into Vero cells as previously described [41]. The recovered viruses rDENV-1-NS4B-116A, rDENV-1-NS4B-116M and rDENV-1-NS4B-116V were titrated for further experiments. The sequences of the recombinant viruses were checked for no other nucleotide mutation.

Analysis of focus and plaque forming morphology and *in vitro* growth kinetics

To determine the focus and plaque morphology of viruses, a 24 well plate with 80% confluent Vero cell monolayer was infected with a serial tenfold dilution of virus. After 2hrs incubation, the monolayer was overlaid with 1.25% methylcellulose in MEM and then the plate was incubated 6 days for focus forming assay (FFA) and 9 days for plaque forming assay (PFA)

To determine the viral growth kinetics comparison, three recombinant viruses rDENV-1-NS4B-116A, rDENV-1-NS4B-116M, and rDENV-1-NS4B-116V were infected to C6/36 and Vero cells at MOI (multiplicity of infection) of 0.01, Hep G2, immature iPS-ML-DCs cells at

MOI of 0.1 and K-562 cells at MOI of 5. The culture fluids containing the viruses were harvested at different time points and virus titration was done by FFA on Vero cells.

Virus fitness competition assay

This method was modified from the protocols of Cioat *et al.* [21] and Coffey *et al.*[4]. A mixture of two virus strains rDENV-1-NS4B-116A versus rDENV-1-NS4B-116V and rDENV-1-NS4B-116M versus rDENV-1-NS4B-116V were infected in duplicate wells containing HepG2 and C6/36 cells at a concentration of 5×10^5 cells/well. The ratio rDENV-1-NS4B-116A/M: rDENV-1-NS4B-116V in the mix inoculated to HepG2 cells and C6/36 cells were fixed to 1:10 and 10:1, respectively (calculation based on genome copies). Culture supernatants collected at 4 days p.i. were then passaged serially in the same cell line for up to 3 passages. The titre of the virus inoculated in all passages was maintained at 10^6 genome copies. For all passages, cells were incubated for at 4 days. The proportion of the clone rDENV-1-NS4B-116A/M in the virus populations in each passage was determined by using 3D-digital PCR assay. The proportion of the clone rDENV-1-NS4B-116V was calculated by using the formula (100% - x% of mutant clone). The results were confirmed with Sanger sequencing by determining the height of the nucleotide encoding either 116Val (codon GTG) or 116Ala/Met (codon GCG/ATG) [4]. A single recombinant virus was also included as a control for tracking of any mutation that might appear during passaging of cell lines.

RNA isolation, preparation for microarray and data analysis

Immature iPS-ML-DCs cells and HepG2 cells were seeded at a total number of 10^6 cells and then were infected with three recombinant virus clones at MOI 0.1. At the time points of 5 min, 30 min and 24 h, 48 h p.i., the infected culture fluids were harvested and cells were washed twice with ice-cold PBS. The cells were then lysed by using 700 μ l TRI reagent (MRC, Montgomery Rd Cincinnati, OH). Total RNA was extracted from the lysed cell by using Direct-zol RNA MicroPrep kit (Zymo Research, USA). Fluorescent labeling-cRNA

samples were prepared from 200 ng of extracted RNA by using The Low Input QuickAmp Labeling Kit, One-Color kit (Agilent, TX) according to the manufacturer's protocol.

GeneSpring GX software (Agilent, USA) was used to analyze the statistical test. One way ANOVA followed by Benjamini-Hochberg correction was performed. Fold-change analyses were then performed against the three virus clones and a 2-fold cut-off as compared to the control was used. Hierarchical clustering of all samples at various time points was built by comparing to the control.

Determination of IFN levels

The supernatants from infected iPS-ML-DCs cells above were collected and subjected to the ELISA assays for the quantification of human IFN- α (R&D system, USA) and human IFN- β (MyBiosource, USA). The fold change was calculated by a formula:

$$\left[\frac{\text{concentration of IFN secreted from cells infected with rDENV-1-NS4B-116A/M}}{\text{concentration of IFN secreted from cells infected with rDENV-1-NS4B-116V}} \right]$$

Author statements

Funding information

This work was supported by grants from the Japan Initiative for Global Research Network on Infectious Diseases (JGRID) of the Japan Science and Technology Agency (JST); e-Asia Joint Research Program (e-Asia JRP) and Research Program on Emerging and Re-emerging Infectious Diseases of the Agency for Research and Development (AMED).

Funders have no role in the study design, data collection, and interpretation, or the decision to submit this work for publication.

Acknowledgments

We would like to acknowledge Dr. Satoru Senju -Department of Immunogenetics, Kumamoto University Graduate School of Medical Sciences for providing the iPS-ML cells. We would like to thank Corazon C. Buerano, Ferdinard Adungo, all staff, and members of the Department of Virology, NEKKEN, Nagasaki University, Japan for providing technical support and advice.

Conflicts of interest

The authors declare that there are no conflicts of interest.

Ethical statement

Informed consent was obtained from all patients before sampling. This study protocol was approved by the Ethics Committee of National Institute of Hygiene and Epidemiology, Vietnam (no.IRB-VN01059-17) and the Institute of Tropical Medicine, Nagasaki University, Japan (no.08061924).

Abbreviations

DEGs: Differentially Expressed Genes

IFN: interferon

iPS-ML: iPS cell-derived myeloid cell line

iPS-ML-DC: iPS cell-derived DC-like cell

ISGs: Interferon-stimulated genes

MEM: Minimum Essential Medium

MOI: multiplicity of infection

FCS: Fetal Calf Serum

FBS: Fetal Bovine Serum

FFA: Focus Forming Assay

FFU: Focus Forming Unit

p1-p7: passage 1 to passage 7

PBS: Phosphate Buffered Saline

PFA: Plaque Forming Assay

RPMI: Roswell Park Memorial Institute medium

RT-PCR: Reverse Transcription-Polymerase Chain Reaction

STAT-1: Signal transducer and activator of transcription 1

References

1. **Lindenbach BD, Rice, C.M.** Flaviviridae: Flavivirus. In: Knipe DM, Howley, P.M (editor). *Fields Virology*. Philadelphia: Lippincott Williams & Wilkins; 2013. pp. 712-747.
2. **Zmurko J, Neyts J, Dallmeier K.** Flaviviral NS4b, chameleon and jack-in-the-box roles in viral replication and pathogenesis, and a molecular target for antiviral intervention. *Rev Med Virol* 2015;25(4):205-223.
3. **Lauring AS, Andino R.** Quasispecies theory and the behavior of RNA viruses. *PLoS Pathog* 2010;6(7):e1001005.
4. **Coffey LL, Beeharry Y, Borderia AV, Blanc H, Vignuzzi M.** Arbovirus high fidelity variant loses fitness in mosquitoes and mice. *Proc Natl Acad Sci U S A* 2011;108(38):16038-16043.
5. **Coffey LL, Vasilakis N, Brault AC, Powers AM, Tripet F et al.** Arbovirus evolution in vivo is constrained by host alternation. *Proc Natl Acad Sci U S A* 2008;105(19):6970-6975.
6. **Lanciotti RS, Lewis JG, Gubler DJ, Trent DW.** Molecular evolution and epidemiology of dengue-3 viruses. *J Gen Virol* 1994;75 (Pt 1):65-75.
7. **Weaver SC, Brault AC, Kang W, Holland JJ.** Genetic and fitness changes accompanying adaptation of an arbovirus to vertebrate and invertebrate cells. *J Virol* 1999;73(5):4316-4326.
8. **Lin SR, Hsieh SC, Yueh YY, Lin TH, Chao DY et al.** Study of sequence variation of dengue type 3 virus in naturally infected mosquitoes and human hosts: implications for transmission and evolution. *J Virol* 2004;78(22):12717-12721.
9. **Kurosu T.** Quasispecies of dengue virus. *Trop Med Health* 2011;39(4 Suppl):29-36.
10. **Kinoshita H, Mathenge EG, Hung NT, Huong VT, Kumatori A et al.** Isolation and characterization of two phenotypically distinct dengue type-2 virus isolates from the same dengue hemorrhagic Fever patient. *Jpn J Infect Dis* 2009;62(5):343-350.
11. **Wang WK, Lin SR, Lee CM, King CC, Chang SC.** Dengue type 3 virus in plasma is a population of closely related genomes: quasispecies. *J Virol* 2002;76(9):4662-4665.
12. **Lescar J, Luo D, Xu T, Sampath A, Lim SP et al.** Towards the design of antiviral inhibitors against flaviviruses: the case for the multifunctional NS3 protein from Dengue virus as a target. *Antiviral Res* 2008;80(2):94-101.
13. **Noble CG, Seh CC, Chao AT, Shi PY.** Ligand-bound structures of the dengue virus protease reveal the active conformation. *J Virol* 2012;86(1):438-446.
14. **Xie X, Zou J, Wang QY, Shi PY.** Targeting dengue virus NS4B protein for drug discovery. *Antiviral Res* 2015;118:39-45.
15. **W.H.O.** Epidemiology, burden of disease and transmission. *Dengue: Guidelines for diagnosis, treatment, prevention and control-New edition*. France: WHO Health Organization; 2009. pp. 3-17.
16. **Wang WK, Sung TL, Tsai YC, Kao CL, Chang SM et al.** Detection of dengue virus replication in peripheral blood mononuclear cells from dengue virus type 2-infected patients by a reverse transcription-real-time PCR assay. *J Clin Microbiol* 2002;40(12):4472-4478.
17. **Jessie K, Fong MY, Devi S, Lam SK, Wong KT.** Localization of dengue virus in naturally infected human tissues, by immunohistochemistry and in situ hybridization. *J Infect Dis* 2004;189(8):1411-1418.

18. **Thant KZ, Morita K, Igarashi A.** Detection of the disease severity-related molecular differences among new Thai dengue-2 isolates in 1993, based on their structural proteins and major non-structural protein NS1 sequences. *Microbiol Immunol* 1996;40(3):205-216.
19. **Wang WK, Sung TL, Lee CN, Lin TY, King CC.** Sequence diversity of the capsid gene and the nonstructural gene NS2B of dengue-3 virus in vivo. *Virology* 2002;303(1):181-191.
20. **Sim S, Aw PP, Wilm A, Teoh G, Hue KD et al.** Tracking Dengue Virus Intra-host Genetic Diversity during Human-to-Mosquito Transmission. *PLoS Negl Trop Dis* 2015;9(9):e0004052.
21. **Ciota AT, Lovelace AO, Ngo KA, Le AN, Maffei JG et al.** Cell-specific adaptation of two flaviviruses following serial passage in mosquito cell culture. *Virology* 2007;357(2):165-174.
22. **Orozco S, Schmid MA, Parameswaran P, Lachica R, Henn MR et al.** Characterization of a model of lethal dengue virus 2 infection in C57BL/6 mice deficient in the alpha/beta interferon receptor. *J Gen Virol* 2012;93(Pt 10):2152-2157.
23. **Ciota AT, Kramer LD.** Insights into arbovirus evolution and adaptation from experimental studies. *Viruses* 2010;2(12):2594-2617.
24. **Jenkins GM, Rambaut A, Pybus OG, Holmes EC.** Rates of molecular evolution in RNA viruses: a quantitative phylogenetic analysis. *J Mol Evol* 2002;54(2):156-165.
25. **Zanotto PM, Gould EA, Gao GF, Harvey PH, Holmes EC.** Population dynamics of flaviviruses revealed by molecular phylogenies. *Proc Natl Acad Sci U S A* 1996;93(2):548-553.
26. **Hanley KA, Manlucu LR, Gilmore LE, Blaney JE, Jr., Hanson CT et al.** A trade-off in replication in mosquito versus mammalian systems conferred by a point mutation in the NS4B protein of dengue virus type 4. *Virology* 2003;312(1):222-232.
27. **Umareddy I, Chao A, Sampath A, Gu F, Vasudevan SG.** Dengue virus NS4B interacts with NS3 and dissociates it from single-stranded RNA. *J Gen Virol* 2006;87(Pt 9):2605-2614.
28. **Zou J, Xie X, Wang QY, Dong H, Lee MY et al.** Characterization of dengue virus NS4A and NS4B protein interaction. *J Virol* 2015;89(7):3455-3470.
29. **Miller S, Sparacio S, Bartenschlager R.** Subcellular localization and membrane topology of the Dengue virus type 2 Non-structural protein 4B. *J Biol Chem* 2006;281(13):8854-8863.
30. **Li Y, Kim YM, Zou J, Wang QY, Gayen S et al.** Secondary structure and membrane topology of dengue virus NS4B N-terminal 125 amino acids. *Biochim Biophys Acta* 2015;1848(12):3150-3157.
31. **Li Y, Wong YL, Lee MY, Li Q, Wang QY et al.** Secondary Structure and Membrane Topology of the Full-Length Dengue Virus NS4B in Micelles. *Angew Chem Int Ed Engl* 2016;55(39):12068-12072.
32. **Blaney JE, Jr., Hanson CT, Firestone CY, Hanley KA, Murphy BR et al.** Genetically modified, live attenuated dengue virus type 3 vaccine candidates. *Am J Trop Med Hyg* 2004;71(6):811-821.
33. **Tajima S, Takasaki T, Kurane I.** Restoration of replication-defective dengue type 1 virus bearing mutations in the N-terminal cytoplasmic portion of NS4A by additional mutations in NS4B. *Arch Virol* 2011;156(1):63-69.

34. **Munoz-Jordan JL, Laurent-Rolle M, Ashour J, Martinez-Sobrido L, Ashok M et al.** Inhibition of alpha/beta interferon signaling by the NS4B protein of flaviviruses. *J Virol* 2005;79(13):8004-8013.
35. **Munoz-Jordan JL, Sanchez-Burgos GG, Laurent-Rolle M, Garcia-Sastre A.** Inhibition of interferon signaling by dengue virus. *Proc Natl Acad Sci U S A* 2003;100(24):14333-14338.
36. **Schoggins JW, Rice CM.** Interferon-stimulated genes and their antiviral effector functions. *Curr Opin Virol* 2011;1(6):519-525.
37. **Youn S, Li T, McCune BT, Edeling MA, Fremont DH et al.** Evidence for a genetic and physical interaction between nonstructural proteins NS1 and NS4B that modulates replication of West Nile virus. *J Virol* 2012;86(13):7360-7371.
38. **Giraldo MI, Vargas-Cuartas O, Gallego-Gomez JC, Shi PY, Padilla-Sanabria L et al.** K48-linked polyubiquitination of dengue virus NS1 protein inhibits its interaction with the viral partner NS4B. *Virus Res* 2017;246:1-11.
39. **Li S, Yu X, Guo Y, Kong L.** Interaction networks of hepatitis C virus NS4B: implications for antiviral therapy. *Cell Microbiol* 2012;14(7):994-1002.
40. **Haruta M, Tomita Y, Yuno A, Matsumura K, Ikeda T et al.** TAP-deficient human iPS cell-derived myeloid cell lines as unlimited cell source for dendritic cell-like antigen-presenting cells. *Gene Ther* 2013;20(5):504-513.
41. **Tajima S, Nukui Y, Ito M, Takasaki T, Kurane I.** Nineteen nucleotides in the variable region of 3' non-translated region are dispensable for the replication of dengue type 1 virus in vitro. *Virus Res* 2006;116(1-2):38-44.

Figure and table legends

Fig.1. Schematic of *in vitro* passaging experiment with two serum samples VN/2013/Hue 265 (NS4B-116A presented) and VN/2013/Hue 432 (NS4B-116M presented). Cell passage was stopped when the population of NS4B-116A and 116M in two samples both surpassed 50%, at which each variant reached a plateau in the population growth. All passages were carried out at a constant MOI of 0.1.*: The passage of VN/2013/Hue/432 was stopped. **: The passage of VN/2013/Hue/265 was stopped.

Fig.2. Comparison of focus and plaque morphologies in cells infected with viruses derived from passages in cell lines. Vero cells were used in the assays.(a,b,c,e). Viruses from sample VN/2013/Hue/265 caused small and homogenous foci of infected cells in terms of size at p1 of C6/36, p1 of Vero cells, p7 of serial passage in C6/36 cells, and p7 of alternate passage between C6/36 and Vero cells, respectively. (d,f). Virus populations at p7 of serial passage in Vero cells and at p7 of alternate passage between Vero and C6/36 cells both produced heterogeneous big foci mixed with smaller ones. (g-i) Virus populations isolated from the sample VN/2013/Hue/432 caused small foci at p1 of C6/36 cells, p1 in Vero cells, and p3 of serial passage in C6/36 cells, respectively. (j) Virus population at p3 of serial passage in Vero cells produced mostly big foci together with smaller ones. (k-m) The focus forming phenotype by focus forming assay and (n-p) plaque forming phenotype by plaque forming assay were compared by using recombinant viruses rDENV-1-NS4B-116A, rDENV-1-NS4B-116M, and rDENV-1-NS4B-116V.

Fig 3. Comparison of the growth kinetics of three virus clones. (a). Two recombinant viruses rDENV-1-NS4B-116A and rDENV-1-NS4B-116M grew less effectively in C6/36 cells (~ 10 times lower at day 6 after infection) compared to rDENV-1-NS4B-116V. (b-d). The opposite trend was seen in human cell lines K-562, immature iPS-ML-DCs and Hep G2 cells in which the two mutant rDENV-1-NS4B-116A/M viruses clones grew approximately 10 times higher than rDENV-1-NS4B-116V clone. The differences are significant. (e). In Vero cells, three strains showed the same growth patterns. All experiments were done in triplicates and each value represents mean of \log_{10} (f.f.u.ml⁻¹ titre) \pm SD. The p-values were calculated by unpaired t-test using GraphPad Prism 6. * indicates $P < 0.05$.

Fig. 4. The competition fitness assays. *: the square represents the virus clone rDENV-1-NS4B-116A/M, **: the triangle represents the virus clone rDENV-1-NS4B-116V. An inoculation mixture of two virus clones rDENV-1-NS4B-116A and rDENV-1-NS4B-116V;

rDENV-1-NS4B-116M and rDENV-1-NS4B-116V were co-infected to HepG2 and C6/36 cells. The ratio NS4B-116A/M: NS4B-116V in the mixture was fixed to 1:10 in HepG2 cells, and 10:1 in C6/36 cells (calculation was based on genome copies). The infected culture fluids harvested at 4 days p.i. were sub-inoculated in the same cell lines for a maximum of 3 passages. (a-d). The bar charts show the percentage of each clone in the original mixture and in each passage in HepG2 and C6/36 cells. The experiments were carried out in at least two replicates and each value represents the mean percentage \pm standard deviation (Mean \pm SD)

Fig.5. Transcriptional signature analysis. (a) Heat map of 112 genes that were differentially expressed in infected samples compared to the control. (b) Expression heat map of close-related genes derived from cluster I. (c) Expression heat map of close-related genes derived from cluster II. (d-f) Bar charts show fold change (compared to the control) of important genes which were differentially expressed in the cells infected with rDENV-1-NS4B-116A, rDENV-1-NS4B-116M and rDENV-1-NS4B-116V at 5 min p.i., 30 min p.i. and 24 h p.i. (g-h) The bar chart shows the fold change of IFN α/β levels produced by iPS-ML-DCs infected with rDENV-1-NS4B-116A/M over those with rDENV-1-NS4B-116V at indicated time points after infection. The p-values were calculated by unpaired t-test using GraphPad Prism 6. ** indicates $P < 0.01$.

Fig. 6. (a). The topology of the DENV-2 non-structural protein NS4B according to published data [29-31]. (b). Alignment of DENV NS4B of all four serotypes. The alignment was performed by using CLC sequence viewer. The arrows represent the variants in the pTMD3 of NS4B. The residue 116Valine is conserved between DENV-1 (sample VN/2013/Hue/265, GenBank accession no. KX595191), DENV-2 (AAB58782), DENV-3 (KY863456) and varied in DENV-4 (ARX96505). The residue 116V in DENV-1 is 115V in DENV-2,3 and 112L in DENV-4.

Table 1. Amino acid changes in NS4B region after consecutive passages in Vero cells.

VN/2013/Hue/265				
Amino acid variants at position 116 of DENV-1 NS4B				
Passage	Serial C6/36	Serial Vero	Alternate C6/36 and Vero	Alternate Vero and C6/36
p1	Val	5.1% Ala + 94.9% Val	Val	94.9% Val + 5.1% Ala
p2	Val	32.6% Ala + 67.4% Val	Val	Val
p3	Val	56.2% Ala + 43.8% Val	Val	Val
p5	Val	60.5 % Ala+ 39.5% Val	Val	92.8% Val + 7.2% Ala
p7	Val	67.1% Ala + 32.9% Val	Val	63% Val + 37%Ala
VN/2013/Hue/432				
Amino acid variants at position 116 of DENV-1 NS4B				
Passage	Serial C6/36	Serial Vero	Alternate C6/36 and Vero	Alternate Vero and C6/36
p1	Val	4.6% Met + 95.4% Val	Val	4.6% Met + 95.4% Val
p2	Val	52.9% Met + 47.1% Val	Val	Val
p3	Val	61% Met + 39% Val	Val	Val

Figures

Fig.1

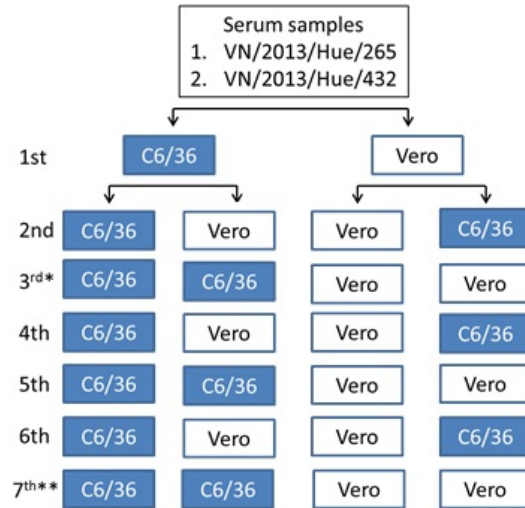


Fig. 2

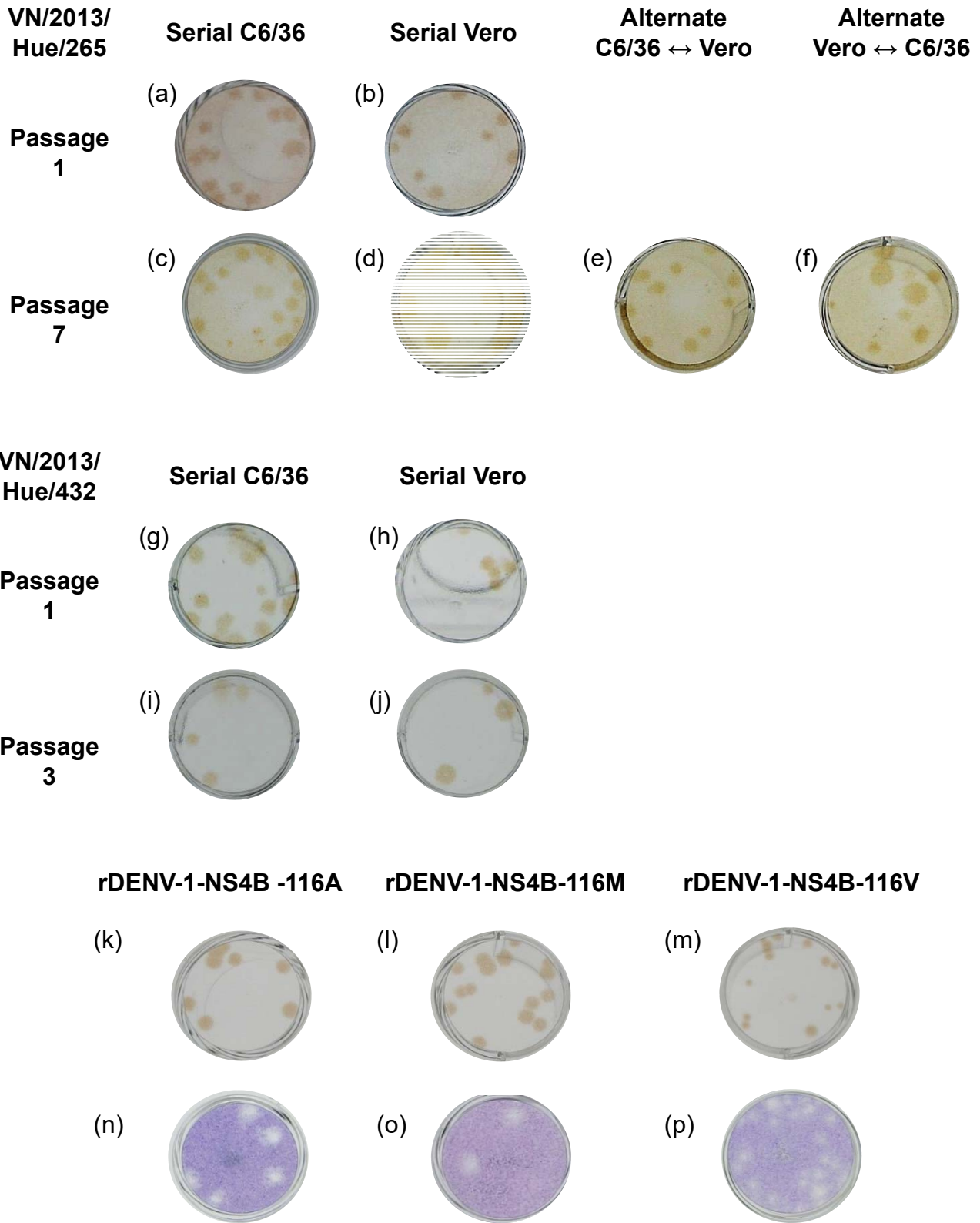


Fig 3

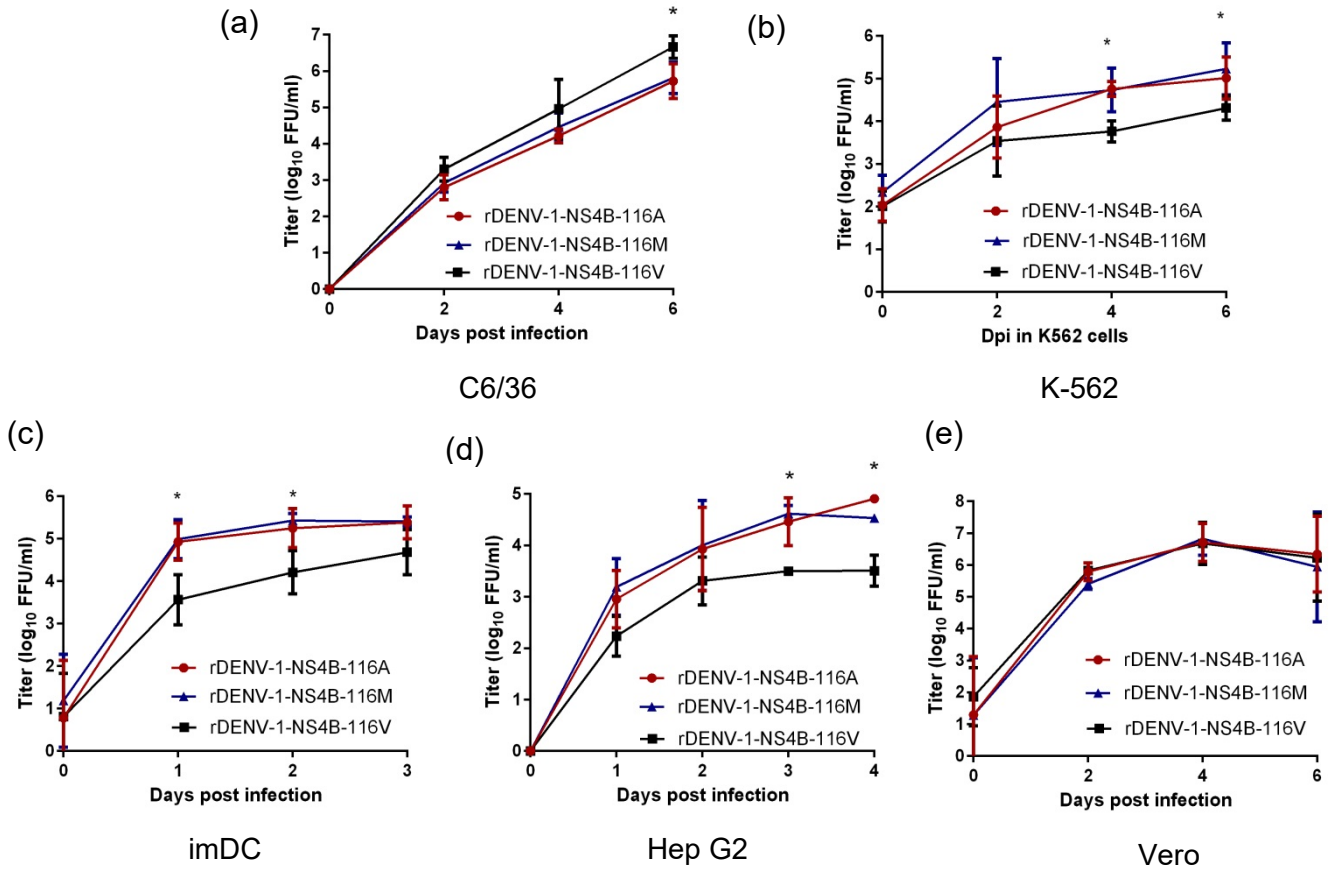


Fig. 4

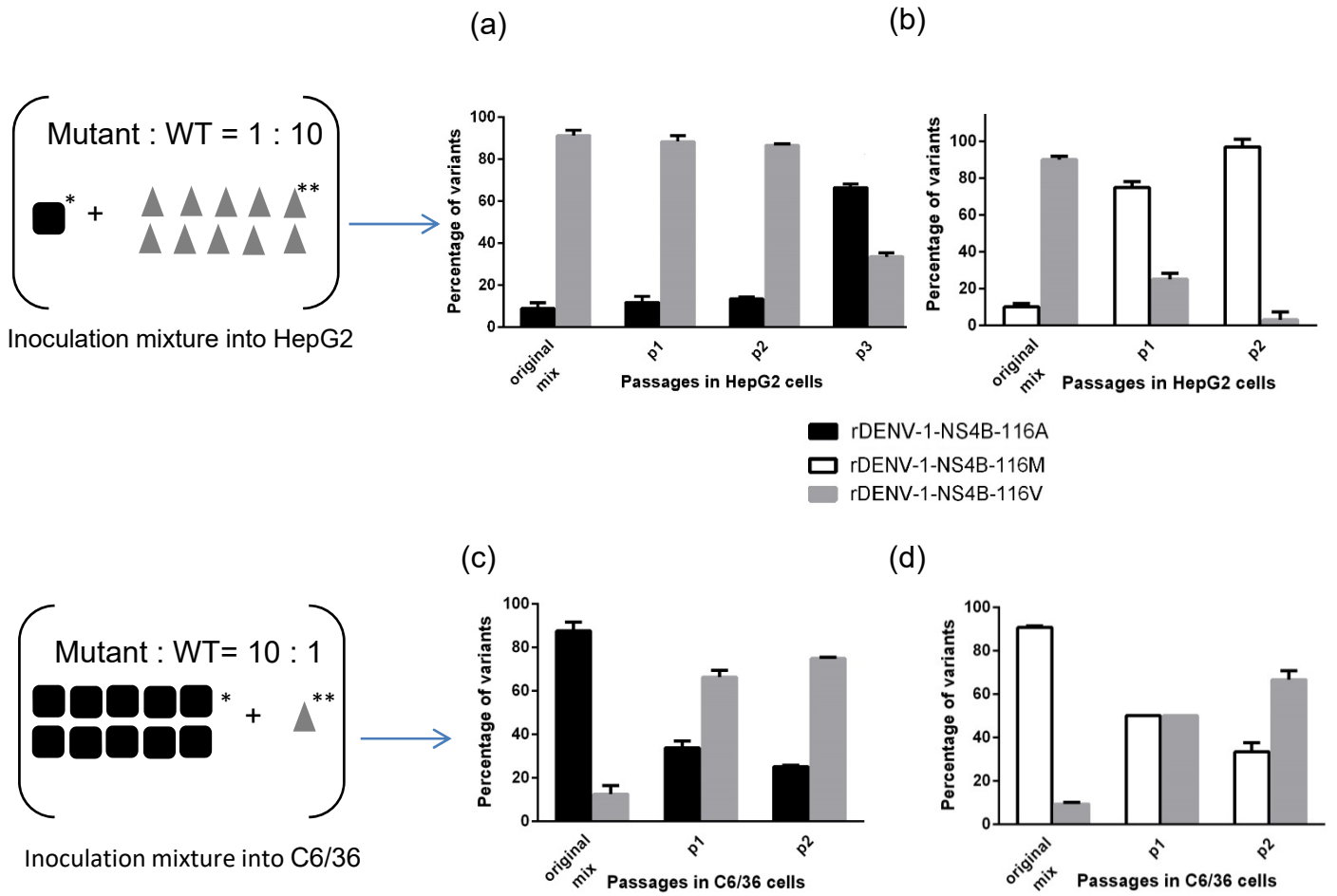


Fig. 5

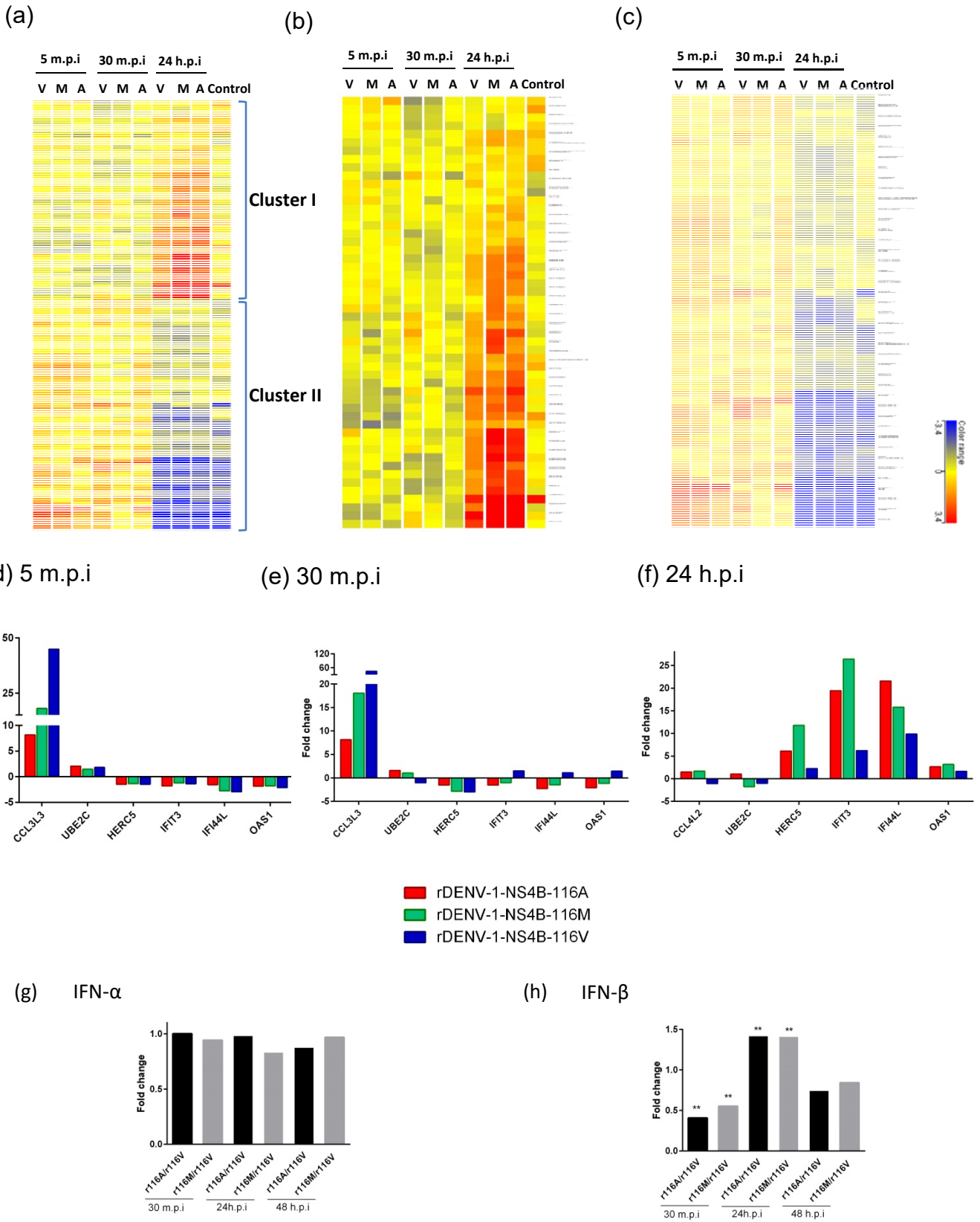
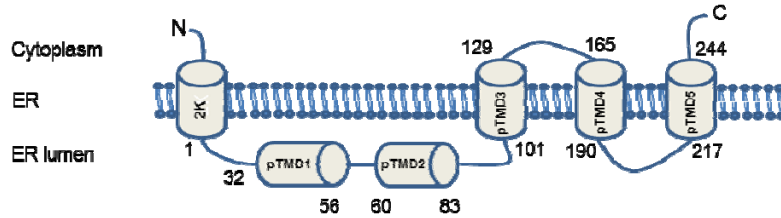


Fig. 6

(a)



(b)

	pTMD1 (residue 32-56)							
	20	40	60					
DENV-1	NEMGLETTK	KDLGI---	G	HVAVENHHHA	AMLDVDLHPA	SAWTLYAVAT	TIITPMMRHT	IENTTANISL
DENV-2	...F..K..	...L----		SI.-TQQPES	NI..I..R..FV...L..S	...SSV.V..
DENV-3	R...MSKEP	V.SPTSY--	-----V...L...	...S...V..
DENV-4I.K..	T.F.F----	Y	Q.K-T---ET	TI.....R..L...L...	...S..L..

	pTMD2 (residue 60-83)				pTMD3 (residue 101-129)			
	80	100	120	140				
DENV-1	TAIANQAAIL	MGLDKGWPI	S	KMDIGVPLLA	LGCYSQVNPL	TLTAAVLMLV	AHYAIIGPGL	QAKATREAQK
DENV-2TV.	...G...L.ILFL..
DENV-3	A.....VV.L.....L..T
DENV-4	A.....V.	...G...LH	R..L.....	M.....T	...SLV..L	V.....

	pTMD4 (residue 165-190)						
	160	180	200	220			
DENV-1	RTAAGIMKNP	TVDGIVAIDL	DPVVYDAKFE	KQLGQIMLLI	LCTSQILLMR	TTWALCESIT	LATGPLTLTW
DENV-2	.A.....	...TV...	..IP..P...	...V...V	..VT.V.M..AL.	...IS...
DENV-3MT...	...I..S...	...V...V	..AV.L...	..S..F..AL	...I...
DENV-4TV...	E..IS..P...	...V...V	..AG.L...	...F..VL.	...IL...

	pTMD5 (residue 217-244)				
	220	240			
DENV-1	EGSPGKFWNT	TIAVSMANIF	RGSYLAGAGL	AFSLMKSLGG	GRRGTGAQ
DENV-2	..N..R....	L..I..NTTN	T.....NI
DENV-3I...V.T	.K....S.
DENV-4	..N..R....T....I.NVQT	P.....TT

Supplements

Fig. S1: Sample VN/2013/Hue/265: (a-c). Nucleotide change of NS4B-116 in virus population at p1, p3, and p7 of serial passages in Vero cells. (d). The proportion of variant NS4B-116A in p1-p7 of serial passages in Vero cells. Sample VN/2013/Hue/432: (e-g). Nucleotide change of NS4B-116 in virus population at p1, p2, and p3 of serial passages in Vero cells. (h) The proportion of variant NS4B-116M in p1-p3 of serial passages in Vero cells. All the quantifications were conducted by 3D-digital PCR assay. The results were presented as mean of percentage \pm standard deviation (Mean \pm SD). (i-k) Nucleotide change of NS4B-116 in virus population of samples VN/2013/Hue/265 at p3, p5, and p7 of alternate passage between Vero and C6/36 cells.

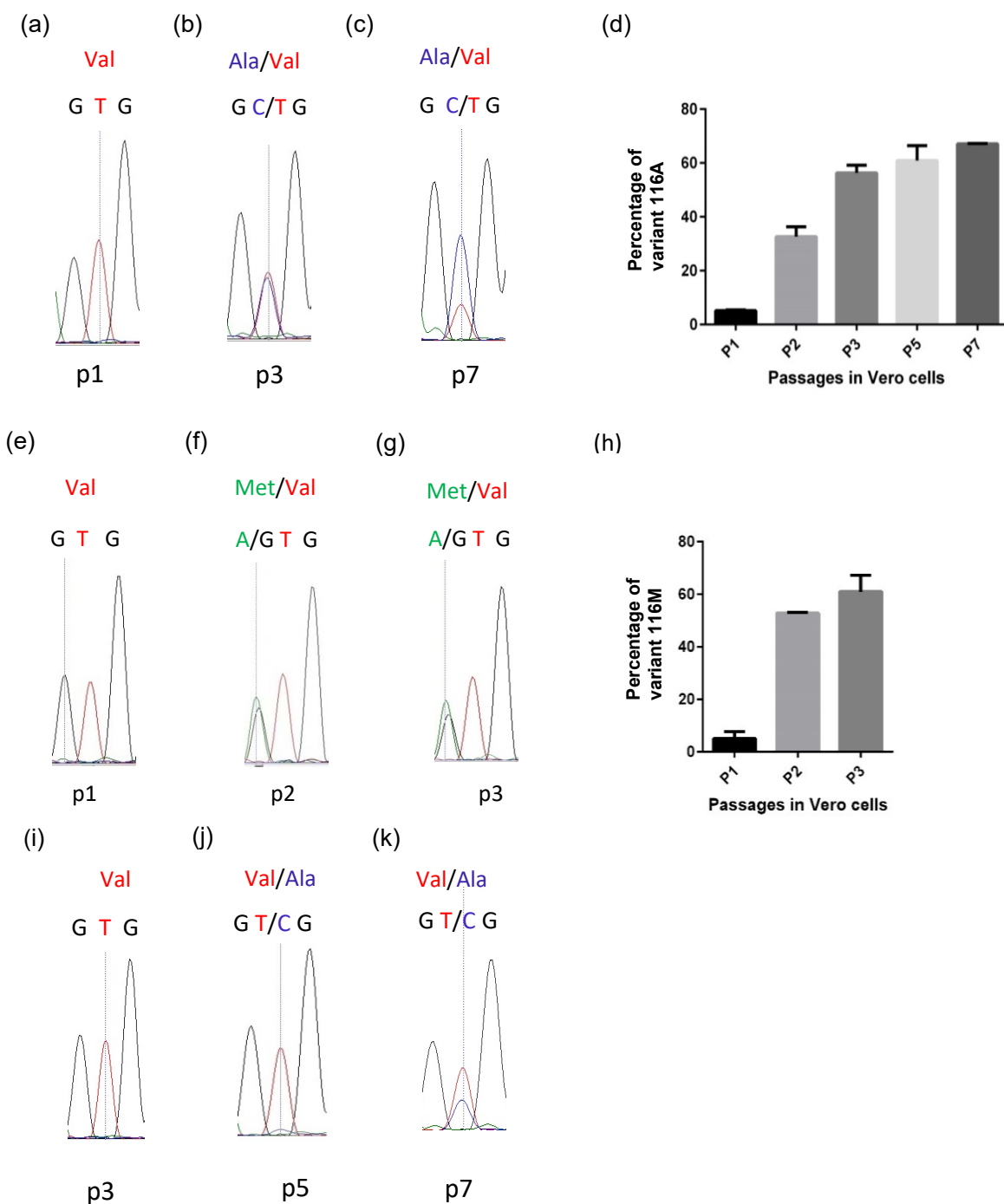


Table S1. Amino acid variants in the DENV-1 isolated from dengue patients

Strain (VN/2013/Hue)	Passage	Cell line	Amino acid position	Amino acid change	Changed codon (nucleotide)	Conserved codon
32	2	Vero	20 NS2B	Met	ATG	ATA (Ile)
265	3	Vero	116 NS4B	Ala	GCG	G TG (Val)
265	3	C6/36	116 NS4B	Val	G TG	G TG (Val)
338	3	Vero	116 NS4B	Met	ATG	G TG (Val)
338	3	C6/36	116 NS4B	Val	G TG	G TG (Val)
387	3	Vero	116 NS4B	Met	ATG	G TG (Val)
387	3	C6/36	116 NS4B	Val	G TG	G TG (Val)
432	2	Vero	116 NS4B	Met	GCG	G TG (Val)
432	2	C6/36	116 NS4B	Val	G TG	G TG (Val)
762	2	Vero	116 NS4B	Met	ATG	G TG (Val)
762	2	C6/36	116 NS4B	Val	G TG	G TG (Val)
817	2	Vero	116 NS4B	Met	ATG	G TG (Val)
817	2	C6/36	116 NS4B	Val	G TG	G TG (Val)
817	2	Vero	109 NS4A	Ser	TCC	TTC (Phe)
988	2	Vero	81 prM	Arg	CGA	CAA (Gln)
988	2	C6/36	116 NS4B	Val	G TG	G TG (Val)
988	2	Vero	116 NS4B	Met	GCG	G TG (Val)

Table S2. Primers and probes used in the study

Primers	Sequence (5'-3')
Denv1NS4B 6948F	TCTATGCAGTGGCCACAACA
Denv1NS4B 7498R	GTTTGCCATGGACACCGCTA
Denv consensus F	TCAATATGCTGAAACGCGCGAGAAACCG
Denv consensus R	TTGCACCAACAGTCAATGTCTTCAGGTTTC
Denv1E-std 1181F	TGTGTGTCGACGAACGTTTGTGGA
Denv1E-std 2980R	CCAGTACCCCATGTCAGCGTG
Denv1E-1381F	GAACATGGRACAAYTGCAACYAT
Denv1E-1426R	CCGTAGTCDGTCAGCTGTATTTCA
Denv1 1405E probe	FAM-ACACCTCAAGCTCC-3'MGB
Denv1NS4B-7117F	CCACTGACGCTGACAGCG
Denv1NS4B-7181R	GCTTCTCTAGTAGCTTTTGCTTGCA
Denv1NS4B-mut116A probe	FAM-TTGATGCTAGCGGCTCA-MGB(NFQ)
Denv1NS4B-mut116M probe	FAM-TTGATGCTAATGGCTCA-MGB(NFQ)
Denv1NS4B-wt116V 1probe	VIC-TTGATGCTAGTGGCTCA-MGB (NFQ)
Denv1NS4B mut116A 7137F	GGTATTGATGCTAGCGGCTCATTATGCCAT
Denv1NS4B mut116A 7137R	ATGGCATAATGAGCGACTAGCATCAATACC
Denv1NS4B mut116M 7137F	GGTATTGATGCTAATGGCTCATTATGCCAT
Denv1NS4B mut116M 7137R	ATGGCATAATGAGTAAGTACTAGCATCAATACC
For whole genome sequencing	
Denv1 3F1.1	TGTTAGTCTACGTGGACCGACAAGA
Denv1 422 F1.2	CCTACAGCCTTGGCGTTCCATTT
Denv1 701 F1.3	GACAAACGTTCCGTCGCACTGG
Denv1 1057 F1.4	GACATTGAACTCTTGAAGACGGAAG
Denv1 1482 R1	CGCTATAAGGGTGCACATGTTGACA
Denv1 1204 F2.0	TGTGTGTCGACGAACGTTTGTGGA
Denv1 1583 F2.1	CCACTGCCTTGGACCTCGG
Denv1 1909 F2.2	TACGAAGGAACAGATGCACCATGCAA
Denv1 2207 F2.3	ATAGGAGGAGTGTTACGTCTGTTG
Denv1 2484 F2.4	CAATGAAGTTCACACTTGGACAGAGC
Denv1 3001 R2	CCAGTACCCCATGTCAGCGTG
Denv1 2791 F3.1	AGGGGCAGATGTACAGAACACCA
Denv1 3215 F3.2	GGCCGTGGCACCTAGGCAA
Denv1 3580 F3.3	ACACTGGCTGTGTTCTTCTTCTCA
Denv1 3966 F3.4	CATGGAAGACAATGGCTATGGTACTG
Denv1 4500 R3	CTCCAGATCTCTGTTTCTTTTCTGCC
Denv1 4301 F4.1	GAGGTCTCCTGGGAAGAAGAAGC
Denv1 4796 F4.2	AAGAAGTGCAGGTGATTGCTGTTG
Denv1 5100 F4.3	TACATCCAGGATCGGGGAAAACAAG
Denv1 5482 F4.4	TCAGTGGAGGCCTTTCCACAGA
Denv1 6051 R4	CTGCACTCTTTTCTCTCTCTGGCT
Denv1 5643 F5.1	GCTTAAGAAAGAATGGGAAACGGGTG
Denv1 5941 F5.2	CTACATGGGACAGCCTTTAAACAACG
Denv1 6298 F5.3	ACCCCGCTGGCTGGATGC
Denv1 6971 F5.4	ATCACTCCCATGATGAGGCACAC
Denv1 7503 R5	GCTCCTGCTAGATAACTTCCTCTGA
Denv1 7234 F6.1	AAGGACAGCGGCCGGAATAATGAAA
Denv1 7801 F6.2	AGTCATAGACCTCGGTTGTGGAAGA
Denv1 8118 F6.3	TGAATCCCTACATGCCAAGTGTGG
Denv1 8432 F6.4	CACAAGTCAACATGGCATTATGATGAGG
Denv1 8754 F6.5	CAAGAGAGGAGTTCACAAGAAAAGTTAG
Denv1 9232 R6	GCATGTTTCGGGTTCCATGATGTCA
Denv1 8600 F7.1	ACTGACACTACACCCTTTGGACAAC

Denv1 8934 F7.2	TGGGGAAGAGAGAGAGAAAAAGCTAGG
Denv1 9328 F7.3	TGGAACCGTGATGGATGTCATATCC
Denv1 9664 F7.4	AGGATGGAATGATTGGCAACAAGTGC
Denv1 9978 F7.5	GGATGACAACAGAAGACATGCTGTC
Denv1 10309 F7.6	TCAAACAAGGCAAGAAGTCAGGCC
Denv1 10709 R7	AGAACCTGTTGATTCAACAGCACCATT

Table S3: The fold change ≥ 2 of three rDENV-1 infected samples over the control at various time points

a. iPS-ML-DC cells

Notes : Fold change ≥ 2.0

#Entity List : Oneway ANOVA p (Corr) cut-off = 0.05

#Interpretation : strain - time

#Experiment : Dendritic DENV

#Fold-Change cut-off : 2.0

#Pairing option : All against single condition

#Condition pairs :

#[a-24h] vs [Neg-control]

#[a-30m] vs [Neg-control]

#[a-5m] vs [Neg-control]

#[m-24h] vs [Neg-control]

#[m-30m] vs [Neg-control]

#[m-5m] vs [Neg-control]

#[v-24h] vs [Neg-control]

#[v-30m] vs [Neg-control]

#[v-5m] vs [Neg-control]

#Minimum number of pairs:1 out of 9 condition pairs.

Technology : Agilent.SingleColor.72363

Owner : gxuser

GenbankAccession	GeneSymbol	FC ([a-24h] vs [Neg-control])	FC ([m-24h] vs [Neg-control])	FC ([v-24h] vs [Neg-control])	FC ([a-30m] vs [Neg-control])	FC ([m-30m] vs [Neg-control])	FC ([v-30m] vs [Neg-control])	FC ([a-5m] vs [Neg-control])	FC ([m-5m] vs [Neg-control])	FC ([v-5m] vs [Neg-control])	GeneName	ProbeName
NM_002164	IDO1	2.791	7.206	2.062	-1.186	1.052	1.506	-1.306	-1.137	1.381	indoleamine 2,3-dioxygenase 1	A_23_P112026
NM_181801	UBE2C	1.014	-1.756	-1.017	1.601	1.041	-1.032	2.081	1.485	1.820	ubiquitin-conjugating enzyme E2C	A_24_P297539
NM_004417	DUSP1	-2.893	-8.695	-3.370	8.668	3.880	5.043	9.752	4.530	6.613	dual specificity phosphatase 1	A_23_P110712
NM_002534	OAS1	2.646	3.153	1.658	-2.111	-1.172	1.457	-1.828	-1.781	-2.085	2'-5'-oligoadenylate synthetase 1, 40/46kDa	A_23_P64828
NM_000201	ICAM1	-1.101	-1.719	-1.288	5.446	4.980	7.309	4.438	8.027	8.500	intercellular adhesion molecule 1	A_23_P153320
NM_000594	TNF	1.336	1.914	-1.131	36.439	24.101	36.164	52.034	104.439	119.151	tumor necrosis factor	A_23_P376488

NM_002429	MMP19	-1.698	-3.495	-2.385	2.335	1.675	2.905	3.286	3.359	4.521	matrix metallopeptidase 19	A_23_P203888
NM_001001437	CCL3L3	1.168	1.387	1.172	8.148	18.036	44.907	12.968	12.427	21.338	chemokine (C-C motif) ligand 3-like 3	A_33_P3296181
NM_002982	CCL2	9.449	17.190	5.322	24.811	45.252	75.141	41.783	15.762	28.453	chemokine (C-C motif) ligand 2	A_23_P89431
NM_017523	XAF1	4.113	3.485	2.204	-1.174	-1.477	-1.719	1.077	1.047	-1.136	XIAP associated factor 1	A_24_P557479
NM_000265	NCF1	1.313	1.211	-1.525	-1.003	1.804	2.348	1.044	1.209	1.669	neutrophil cytosolic factor 1	A_33_P3369393
NM_001012410	SGOL1	1.911	2.261	1.777	1.382	-1.018	1.044	1.640	-1.053	1.243	shugoshin-like 1 (S. pombe)	A_23_P29723
NM_001303413	RPRD1A	2.034	2.060	2.058	3.486	3.021	3.660	2.863	2.263	1.886	regulation of nuclear pre-mRNA domain containing 1A	A_33_P3291349
NM_003335	UBA7	2.197	2.174	1.331	-1.193	1.205	1.178	-1.185	1.119	-1.017	ubiquitin-like modifier activating enzyme 7	A_23_P21207
NM_001145031	PLAU	1.794	1.434	1.845	4.364	7.193	7.413	5.005	5.700	7.389	plasminogen activator, urokinase	A_33_P3306146
NM_017523	XAF1	4.274	2.845	2.525	-1.706	-1.069	-1.591	-1.891	-2.015	-1.878	XIAP associated factor 1	A_33_P3258346
NM_000507	FBP1	-1.759	-2.463	-2.429	1.290	-1.331	-1.137	1.650	2.015	1.833	fructose-1,6-bisphosphatase 1	A_23_P257111
NM_032299	DCUN1D5	1.280	1.085	1.264	2.688	2.137	2.273	2.300	1.718	2.111	DCN1, defective in cullin neddylation 1, domain containing 5	A_22_P00004999
NM_014059	RGCC	-1.800	-3.723	-2.028	5.236	3.115	5.627	3.720	3.131	2.630	regulator of cell cycle	A_24_P10137
NM_002983	CCL3	1.018	-1.036	-1.312	17.510	15.859	30.777	28.306	44.210	59.468	chemokine (C-C motif) ligand 3	A_33_P3316273
NM_138456	BATF2	7.841	12.171	2.822	-1.344	-1.382	-1.085	-1.010	1.097	1.843	basic leucine zipper transcription factor, ATF-like 2	A_23_P370682
NM_005168	RND3	1.076	1.033	-1.058	4.302	2.782	3.728	3.825	2.499	2.851	Rho family GTPase 3	A_23_P142849
NM_000417	IL2RA	-4.703	-6.455	-6.069	1.263	-1.478	1.009	-1.057	1.334	1.144	interleukin 2 receptor, alpha	A_23_P127288
NM_004345	CAMP	-2.346	-1.678	-2.391	1.662	-1.305	-1.662	1.679	2.346	1.884	cathelicidin antimicrobial peptide	A_23_P253791
NM_203411	TMEM88	1.279	1.649	1.129	11.766	9.103	12.430	8.514	10.800	20.920	transmembrane protein 88	A_23_P77859
NM_001002029	C4B	3.020	7.540	2.267	1.275	1.426	1.598	1.122	-1.382	1.155	complement component 4B (Chido blood group)	A_23_P42282
BC015447	Inc-CETP-1	1.436	2.567	1.410	12.255	11.447	6.102	6.879	5.851	6.543	Inc-CETP-1:1	A_22_P00003927
NM_002417	MKI67	-1.055	-1.618	-1.004	-1.059	-1.638	-2.025	-1.129	-1.035	-1.118	marker of proliferation Ki-67	A_33_P3374210
NM_006820	IFI44L	21.580	15.817	9.868	-2.291	-1.483	1.114	-1.540	-2.738	-2.913	interferon-induced protein 44-like	A_23_P45871
NM_002456	MUC1	-1.452	-2.069	-1.753	1.612	1.404	1.435	1.338	1.383	1.622	mucin 1, cell surface associated	A_23_P137856
NM_000747	CHRNB1	-1.468	-1.282	-1.783	-2.142	-2.116	-2.160	-1.985	-2.018	-1.942	cholinergic receptor, nicotinic, beta 1 (muscle)	A_23_P207106
NM_014314	DDX58	5.459	6.207	2.136	-1.569	-1.965	-1.325	-1.050	-1.595	-1.154	DEAD (Asp-Glu-Ala-Asp) box polypeptide 58	A_33_P3418170
	XLOC_I2_002033	-1.951	-2.008	-1.736	2.132	1.313	1.162	1.821	1.940	1.680		A_21_P0010890

NM_005252	FOS	-1.158	-2.333	-1.270	34.153	27.327	26.353	20.403	6.951	7.227	FBJ murine osteosarcoma viral oncogene homolog	A_23_P106194
NM_052972	LRG1	1.106	1.110	-1.117	6.362	4.726	6.885	5.997	9.465	12.129	leucine-rich alpha-2-glycoprotein 1	A_23_P50638
NR_024214	SNAR-A3	1.908	1.836	2.034	2.643	2.163	1.812	2.871	3.120	2.927	small ILF3/NF90-associated RNA A3	A_33_P3587376
NM_006187	OAS3	5.959	5.174	3.280	-1.633	1.123	1.229	-1.769	-1.512	-1.842	2'-5'-oligoadenylate synthetase 3, 100kDa	A_24_P335305
NM_001135652	EIF2AK2	1.387	1.334	1.111	-1.127	-1.797	-2.331	-1.309	-1.171	-1.324	eukaryotic translation initiation factor 2-alpha kinase 2	A_33_P3224858
NM_001733	C1R	1.419	1.177	1.008	2.199	1.469	1.725	1.744	2.398	2.354	complement component 1, r subcomponent	A_33_P3393821
NR_038940	SH3PXD2A-AS1	-1.229	-1.168	-1.162	1.762	-1.230	1.213	1.741	2.253	2.113	SH3PXD2A antisense RNA 1	A_21_P0000846
NM_006290	TNFAIP3	-1.044	1.050	-1.456	7.390	9.380	13.250	6.101	10.320	14.456	tumor necrosis factor, alpha-induced protein 3	A_24_P157926
XM_005250193	SAMD9L	2.500	1.402	1.519	-1.077	-1.605	-1.335	1.253	1.102	-1.226	sterile alpha motif domain containing 9-like	A_33_P3264846
AX721088	lnc-BZRAP1-1	2.161	2.367	1.580	6.392	5.448	5.678	4.217	4.350	6.143	lnc-BZRAP1-1:1	A_22_P00002219
NM_032779	CCDC142	1.009	1.132	-1.307	-1.935	-2.225	-2.782	-1.887	-2.056	-2.001	coiled-coil domain containing 142	A_23_P424712
NM_012420	IFIT5	4.628	3.031	2.661	-1.104	-1.289	-1.033	1.099	-1.324	-1.325	interferon-induced protein with tetratricopeptide repeats 5	A_24_P30194
XM_005263742		-2.109	-2.167	-2.101	-1.322	-1.148	-1.221	-1.582	-1.318	-1.346		A_33_P3359856
NM_003641	IFITM1	4.105	5.151	2.464	1.426	1.227	1.319	1.375	1.872	1.551	interferon induced transmembrane protein 1	A_23_P72737
NM_022110	FKBPL	1.253	1.372	1.160	-3.478	-2.627	-3.301	-7.218	-3.469	-6.232	FK506 binding protein like	A_23_P70566
NM_005320	HIST1H1D	-1.529	-2.348	-1.677	-2.181	-2.307	-2.957	-1.321	-1.133	-1.457	histone cluster 1, H1d	A_24_P260639
NM_006398	UBD	-1.400	-3.106	-1.465	1.899	-1.403	-1.132	1.134	1.746	1.424	ubiquitin D	A_23_P81898
NM_005253	FOSL2	-2.225	-3.547	-2.324	2.321	1.865	1.879	1.823	1.866	2.026	FOS-like antigen 2	A_23_P348121
NM_024680	E2F8	-1.362	-1.550	-1.830	-1.707	-3.152	-4.163	1.365	-1.120	-1.345	E2F transcription factor 8	A_23_P35871
NM_016323	HERC5	6.121	11.787	2.248	-1.497	-2.856	-2.994	-1.466	-1.349	-1.450	HECT and RLD domain containing E3 ubiquitin protein ligase 5	A_23_P110196
NM_002003	FCN1	-2.778	-4.323	-2.758	1.266	1.045	1.109	1.379	1.974	1.690	ficolin (collagen/fibrinogen domain containing) 1	A_23_P157879
NM_006346	PIBF1	-1.463	-1.551	-1.453	-2.102	-2.096	-2.103	-2.681	-2.435	-2.989	progesterone immunomodulatory binding factor 1	A_33_P3242493
NM_001291470	CCL4L2	1.096	1.504	-1.296	38.511	29.652	63.614	59.091	109.499	165.138	chemokine (C-C motif) ligand 4-like 2	A_23_P207564
NM_000576	IL1B	1.687	1.548	1.315	129.546	144.814	353.895	132.212	299.033	518.070	interleukin 1, beta	A_23_P79518
NM_032222	FAM188B	1.155	1.139	1.071	2.197	1.342	1.566	1.866	2.697	1.833	family with sequence similarity 188, member B	A_24_P126425
NM_022147	RTP4	4.463	4.128	1.962	-1.877	-2.883	-2.994	-1.710	-1.218	-1.823	receptor (chemosensory)	A_23_P166797

											transporter protein 4	
NM_080657	RSAD2	15.166	29.044	5.065	-1.155	1.696	1.546	1.240	-1.296	-1.368	radical S-adenosyl methionine domain containing 2	A_24_P28722
BC015447	Inc-CETP-1	1.239	-1.225	1.110	13.001	9.255	7.049	6.415	4.503	7.412	Inc-CETP-1:2	A_22_P00024977
NR_002590	SNORA41	1.076	1.152	1.025	1.988	1.911	2.191	2.775	2.389	2.445	small nucleolar RNA, H/ACA box 41	A_21_P0000273
NM_152542	PPM1K	-1.995	-2.182	-2.792	-2.451	-3.825	-4.351	-2.525	-1.822	-2.524	protein phosphatase, Mg2+/Mn2+ dependent, 1K	A_24_P214598
NM_002462	MX1	7.150	9.619	3.234	1.094	-1.371	-1.773	1.038	1.371	1.271	MX dynamin-like GTPase 1	A_23_P17663
NM_017912	HERC6	3.225	6.271	2.750	-1.128	-2.206	-1.922	-2.673	-1.139	-1.407	HECT and RLD domain containing E3 ubiquitin protein ligase family member 6	A_23_P250358
NM_001734	C1S	1.411	-1.253	-1.201	-1.210	-2.146	-1.137	-1.339	1.192	1.082	complement component 1, s subcomponent	A_23_P2492
NM_212481	ARID5A	1.122	-1.355	1.038	2.410	2.308	2.285	2.399	2.878	2.845	AT rich interactive domain 5A (MRF1-like)	A_23_P143016
NM_005101	ISG15	4.170	4.817	2.839	1.325	1.052	-1.074	1.392	1.563	1.508	ISG15 ubiquitin-like modifier	A_23_P819
NM_145641	APOL3	1.706	4.057	1.055	-1.016	-1.095	1.072	-1.339	1.198	1.133	apolipoprotein L, 3	A_24_P416997
NM_033101	LGALS12	2.495	1.539	2.820	1.558	1.646	1.576	1.957	2.327	2.089	lectin, galactoside-binding, soluble, 12	A_23_P139198
NM_001964	EGR1	-1.668	-1.797	-1.944	106.460	22.466	13.451	125.176	121.833	83.823	early growth response 1	A_23_P214080
NR_003003	SCARNA17	-1.733	-2.837	-2.091	1.383	1.013	1.029	1.120	1.114	1.177	small Cajal body-specific RNA 17	A_32_P37592
NM_003955	SOCS3	1.170	-2.340	-1.210	8.357	8.785	11.298	7.732	4.303	10.965	suppressor of cytokine signaling 3	A_23_P207058
NM_018487	TMEM176A	-1.356	-2.301	-1.568	-1.185	-1.045	-1.095	-1.114	-1.103	-1.091	transmembrane protein 176A	A_23_P252082
NM_002371	MAL	-1.927	-3.553	-2.372	-1.161	-1.352	-1.166	-1.236	1.063	-1.102	mal, T-cell differentiation protein	A_23_P17134
BC024905	TPP2	-1.006	-1.271	-1.003	2.638	1.985	3.142	2.604	2.318	2.368	tripeptidyl peptidase II	A_33_P3304754
NM_175571	GIMAP8	2.241	1.476	1.400	-2.302	-2.056	-1.536	-2.188	-1.771	-1.673	GTPase, IMAP family member 8	A_24_P132383
NM_182898	CREB5	-2.650	-2.998	-2.458	-1.268	-1.463	-1.429	-1.056	-1.200	-1.216	cAMP responsive element binding protein 5	A_23_P157117
		1.289	1.179	-1.193	-13.540	-13.696	-9.578	-16.849	-11.596	-9.503		A_33_P3634554
NM_178232	HAPLN3	2.845	3.146	2.170	2.164	2.292	2.486	1.869	2.396	2.774	hyaluronan and proteoglycan link protein 3	A_33_P3259393
NM_014232	VAMP2	1.231	1.469	1.303	-1.764	-1.525	-1.473	-3.256	-4.887	-3.250	vesicle-associated membrane protein 2 (synaptobrevin 2)	A_33_P3213493
NM_002535	OAS2	9.454	4.896	6.392	-1.512	1.171	1.670	-1.934	-1.496	-1.333	2'-5'-oligoadenylate synthetase 2, 69/71kDa	A_33_P3225512
NM_001012967	DDX60L	3.711	2.501	1.576	-1.068	-1.820	-1.227	1.141	1.078	1.230	DEAD (Asp-Glu-Ala-Asp) box polypeptide 60-like	A_23_P30069
NM_032789	PARP10	2.508	1.457	1.457	-1.028	1.035	1.195	-1.116	1.082	-1.032	poly (ADP-ribose) polymerase	A_33_P3398448

											family, member 10	
NM_006770	MARCO	-2.107	-2.742	-2.283	1.098	-1.359	-1.006	1.228	1.578	1.368	macrophage receptor with collagenous structure	A_23_P101992
NM_001202557	CD44	-1.354	-1.558	1.018	3.393	2.771	4.047	2.044	2.147	3.181	CD44 molecule (Indian blood group)	A_21_P0000152
NM_003641	IFITM1	4.401	5.465	2.425	1.353	1.263	1.650	1.270	1.774	1.491	interferon induced transmembrane protein 1	A_33_P3423941
NM_002463	MX2	8.004	11.447	3.102	-1.092	-1.331	1.100	1.002	-1.010	1.032	MX dynamin-like GTPase 2	A_23_P6263
NM_201264	NRP2	1.174	1.731	1.220	3.345	3.724	4.227	2.225	2.125	2.601	neuropilin 2	A_24_P50801
NM_005382	NEFM	-2.382	-2.930	-2.838	1.714	-2.137	-1.296	1.855	1.795	1.540	neurofilament, medium polypeptide	A_33_P3249534
NM_018284	GBP3	2.339	4.074	1.285	-1.409	-1.172	-1.219	-1.167	1.456	1.437	guanylate binding protein 3 inhibitor of DNA binding 2, dominant negative helix-loop-helix protein	A_21_P0010536
NM_002166	ID2	1.327	-1.776	1.158	4.376	4.373	6.252	4.870	5.489	4.841		A_23_P143143
NM_003956	CH25H	1.521	1.493	1.041	7.011	4.551	6.273	8.003	6.482	7.852	cholesterol 25-hydroxylase	A_23_P86470
NR_002739	SNORD56	2.122	1.979	2.032	3.341	2.956	3.039	2.574	2.829	2.913	small nucleolar RNA, C/D box 56	A_21_P0000282
NM_017451	BAIAP2	2.064	1.484	1.590	5.029	4.285	4.411	2.781	3.443	3.446	BAI1-associated protein 2	A_23_P315836
NM_017414	USP18	7.285	8.530	3.068	-1.123	1.062	1.349	-1.020	-1.116	-1.121	ubiquitin specific peptidase 18	A_23_P132159
NM_080801	COL13A1	-1.724	-1.209	-1.952	1.976	-1.185	1.246	2.012	2.205	2.011	collagen, type XIII, alpha 1	A_23_P1331
XR_424398	LOC100507616	1.043	-1.260	-1.023	-1.939	-1.537	-1.891	-1.445	-1.857	-2.312	uncharacterized LOC100507616	A_22_P00004189
NM_001289758	IFIT3	19.433	26.427	6.207	-1.526	-1.017	1.513	-1.803	-1.203	-1.373	interferon-induced protein with tetratricopeptide repeats 3	A_33_P3283611
NM_001001437	CCL3L3	1.391	-1.244	1.191	12.108	23.906	60.115	11.125	21.760	34.701	chemokine (C-C motif) ligand 3-like 3	A_24_P228130
		1.267	1.544	1.131	-1.470	-2.004	-1.729	-1.676	-1.669	-1.947		A_33_P3333187
NM_000600	IL6	2.544	3.782	1.484	40.353	17.455	46.587	52.677	110.984	128.659	interleukin 6	A_23_P71037
NM_139266	STAT1	4.334	3.713	2.259	-1.044	-1.204	-1.077	1.069	1.215	1.118	signal transducer and activator of transcription 1, 91kDa	A_24_P274270
NM_001291470	CCL4L2	1.485	1.697	-1.042	31.031	40.680	108.798	60.332	87.635	148.013	chemokine (C-C motif) ligand 4-like 2	A_33_P3354607
		1.492	1.159	1.332	2.856	2.335	2.073	3.484	4.468	3.753		A_22_P00018349
NM_003546	HIST1H4L	-1.045	-2.008	-1.208	1.209	-1.139	-1.415	1.363	1.764	1.548	histone cluster 1, H4I	A_23_P70480
NM_007224	NXP4	3.243	3.114	2.955	1.077	1.703	1.968	1.350	-1.034	1.076	neurexophilin 4	A_33_P3363245
	Inc-PAFAH1B1-2	1.487	-1.177	1.062	-2.651	-2.161	-2.574	-2.457	-2.083	-2.480	Inc-PAFAH1B1-2:2	A_21_P0009212
NM_001012631	IL32	2.070	1.567	2.025	-1.465	1.934	2.752	-1.463	1.028	1.614	interleukin 32	A_23_P15146
NM_002053	GBP1	8.013	8.841	3.195	1.510	1.442	3.187	1.174	-1.712	1.139	guanylate binding protein 1,	A_23_P62890

											interferon-inducible	
NM_001838	CCR7	-1.557	-1.357	-2.178	1.466	-1.101	1.815	-1.060	1.362	2.190	chemokine (C-C motif) receptor 7	A_23_P343398
NM_017631	DDX60	4.071	2.333	2.195	-1.429	-2.540	-1.280	-1.192	-2.245	-1.814	DEAD (Asp-Glu-Ala-Asp) box polypeptide 60	A_23_P41470

b. HepG2 cells

Notes : Fold change >= 2.0

#Entity List : Oneway ANOVA p (Corr) cut-off = 0.05

#Interpretation : time - strain

#Experiment : HEP DENV

#Fold-Change cut-off : 2.0

#Pairing option : All against single condition

#Condition pairs :

#[30-a] vs [Neg-control]

#[30-m] vs [Neg-control]

#[30-v] vs [Neg-control]

#[48-a] vs [Neg-control]

#[48-m] vs [Neg-control]

#[48-v] vs [Neg-control]

#[5-a] vs [Neg-control]

#[5-m] vs [Neg-control]

#[5-v] vs [Neg-control]

#Minimum number of pairs:1 out of 9 condition pairs.

Technology : Agilent.SingleColor.72363

Owner : gxuser

GenbankAccession	GeneSymbol	FC ([5-a] vs [Neg-control])	FC ([5-m] vs [Neg-control])	FC ([5-v] vs [Neg-control])	FC ([30-a] vs [Neg-control])	FC ([30-m] vs [Neg-control])	FC ([30-v] vs [Neg-control])	FC ([48-a] vs [Neg-control])	FC ([48-m] vs [Neg-control])	FC ([48-v] vs [Neg-control])	GeneName	ProbeName
NM_181801	UBE2C	1.80	2.15	2.28	2.12	1.92	1.80	-2.09	-2.17	-2.47	ubiquitin-conjugating enzyme E2C	A_24_P297539
NM_003368	USP1	2.62	2.73	2.76	3.02	2.65	2.47	-1.65	-1.81	-1.67	ubiquitin specific peptidase 1	A_23_P11652
NM_002534	OAS1	1.08	-1.20	-1.16	-1.38	1.22	-1.26	39.53	34.80	19.60	2'-5'-oligoadenylate	A_23_P64828

												synthetase 1, 40/46kDa	
NM_006435	IFITM2	-1.77	-1.66	-1.66	-1.89	-1.70	-1.54	2.19	1.76	2.22		interferon induced transmembrane protein 2	A_24_P287043
NM_001032731	OAS2	1.13	1.27	1.08	1.06	1.46	1.23	59.13	79.32	41.82		2'-5'-oligoadenylate synthetase 2, 69/71kDa	A_33_P3225522
NM_001547	A_23_P24004	1.27	1.50	-1.51	1.27	1.69	2.01	272.19	230.42	107.82		interferon-induced protein with tetratricopeptide repeats 2	A_23_P24004
XM_006726833	USP41	1.82	2.56	1.81	2.58	1.61	1.63	10.70	13.49	7.81		ubiquitin specific peptidase 41	A_32_P54553
NM_017831	RNF125	2.54	2.56	2.44	2.92	2.55	1.73	-1.10	-1.18	-1.04		ring finger protein 125, E3 ubiquitin protein ligase	A_33_P3257993
NM_004705	PRKRIR	3.18	2.76	2.34	2.52	2.82	1.49	-1.01	1.06	1.23		protein-kinase, interferon- inducible double stranded RNA dependent inhibitor, repressor of (P58 repressor)	A_24_P321411
NM_014176	UBE2T	3.00	3.17	2.76	2.83	3.25	2.20	1.09	1.13	1.05		ubiquitin-conjugating enzyme E2T	A_23_P115482
	Inc-FAM76A- 1	-3.46	-3.58	-3.46	-2.98	-2.69	-2.78	2.04	2.43	2.53		Inc-FAM76A-1:1	A_22_P00006278
NM_213662	STAT3	-2.24	-2.01	-1.75	-1.57	-1.79	-1.26	2.77	3.63	2.66		signal transducer and activator of transcription 3 (acute-phase response factor)	A_23_P100795
NM_000629	IFNAR1	2.26	2.05	2.40	1.86	1.79	1.98	1.03	-1.11	1.03		interferon (alpha, beta and omega) receptor 1	A_33_P3277988
NM_002198	IRF1	1.36	1.61	2.13	-1.01	1.12	1.42	2.13	2.44	1.98		interferon regulatory factor 1	A_23_P41765
NM_005532	IFI27	-1.27	-1.17	-1.07	-1.32	-1.28	-1.15	185.72	202.39	137.51		interferon, alpha-inducible protein 27	A_24_P270460
NM_021034	IFITM3	-1.57	-1.43	-1.41	-1.58	-1.55	-1.43	2.58	2.52	2.33		interferon induced transmembrane protein 3	A_23_P87545
NR_001590	IFITM4P	-1.55	-1.40	-1.33	-1.50	-1.43	-1.30	4.07	3.22	3.54		interferon induced transmembrane protein 4 pseudogene	A_24_P16124
NM_003641	IFITM1	-3.97	-3.54	-3.20	-4.26	-4.26	-3.03	8.56	9.91	5.51		interferon induced transmembrane protein 1	A_23_P72737
NM_001548	IFIT1	3.58	4.45	3.19	2.84	2.83	2.56	147.44	159.90	82.56		interferon-induced protein with tetratricopeptide repeats 1	A_23_P52266
NM_003877	SOCS2	4.86	6.06	6.33	5.57	6.23	6.26	-1.23	-1.44	-1.65		suppressor of cytokine	A_23_P128215

											signaling 2	
NM_016323	HERC5	-6.05	-2.99	-1.89	-2.66	-1.69	-4.05	37.82	38.12	17.28	HECT and RLD domain containing E3 ubiquitin protein ligase 5	A_23_P110196
NM_020771	HACE1	1.82	1.86	1.75	2.02	1.71	1.33	-1.17	-1.21	-1.12	HECT domain and ankyrin repeat containing E3 ubiquitin protein ligase 1	A_23_P250002
NM_003352	SUMO1	2.16	2.47	2.13	2.52	2.28	1.54	-1.03	-1.01	-1.11	small ubiquitin-like modifier 1	A_33_P3318459
NM_001547	IFIT2	1.15	-1.39	-1.67	-1.27	-1.68	-1.54	131.81	151.47	49.67	interferon-induced protein with tetratricopeptide repeats 2	A_24_P304071
NM_002462	MX1	1.91	2.02	1.96	1.74	1.88	2.02	48.33	57.70	34.94	MX dynamin-like GTPase 1	A_23_P17663
NM_017912	HERC6	-2.17	-1.37	1.01	-1.15	-1.45	-1.54	10.46	12.30	7.21	HECT and RLD domain containing E3 ubiquitin protein ligase family member 6	A_23_P250358
NM_003352	SUMO1	2.27	2.45	2.39	2.55	2.43	1.91	-1.34	-1.27	-1.37	small ubiquitin-like modifier 1	A_33_P3318465
NM_005101	ISG15	1.56	1.72	1.71	1.61	1.51	1.65	22.80	25.21	14.41	ISG15 ubiquitin-like modifier	A_23_P819
NM_002176	IFNB1	-1.65	1.75	-2.00	1.23	-2.01	-1.82	23.47	23.37	12.44	interferon, beta 1, fibroblast	A_23_P71774
NM_006417	IFI44	-2.75	-1.73	-2.08	10.53	-1.82	-1.94	42.41	39.99	15.29	interferon-induced protein 44	A_23_P23074
NM_003641	IFITM1	-4.03	-3.85	-3.48	-4.46	-4.37	-2.95	9.02	10.24	5.35	interferon induced transmembrane protein 1	A_33_P3423941
NM_003968	UBA3	2.22	2.03	2.06	2.06	2.07	1.72	1.04	1.22	1.38	ubiquitin-like modifier activating enzyme 3	A_23_P211840
NM_022873	IFI6	-2.53	-2.48	-2.14	-2.61	-2.09	-2.25	62.41	70.12	38.11	interferon, alpha-inducible protein 6	A_23_P201459
NM_003733	OASL	2.23	2.05	2.69	1.40	3.29	1.81	503.71	546.31	227.36	2'-5'-oligoadenylate synthetase-like	A_23_P139786
NM_006084	IRF9	1.36	1.04	1.34	1.06	1.40	1.05	20.71	19.14	18.67	interferon regulatory factor 9	A_23_P65442
NM_001289758	IFIT3	1.56	-1.32	1.34	-1.19	1.06	1.69	121.16	136.56	52.78	interferon-induced protein with tetratricopeptide repeats 3	A_33_P3283611